Neuroimaging in animal models of epilepsy

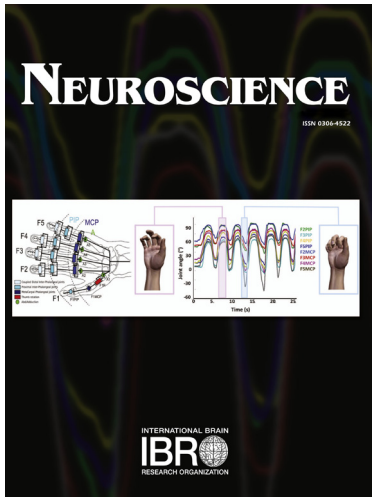

Neuroscience Forefront Review

Neuroimaging in animal models of epilepsy

Daniele Bertoglio, Jeroen Verhaeghe, Stefanie Dedeurwaerdere, Olli Gröhn

PII: S0306-4522(17)30467-0
DOI: http://dx.doi.org/10.1016/j.neuroscience.2017.06.062
Reference: NSC 17874

To appear in: *Neuroscience*

Received Date: 11 April 2017
Revised Date: 27 June 2017
Accepted Date: 28 June 2017

Please cite this article as: D. Bertoglio, J. Verhaeghe, S. Dedeurwaerdere, O. Gröhn, Neuroimaging in animal models of epilepsy, *Neuroscience* (2017), doi: http://dx.doi.org/10.1016/j.neuroscience.2017.06.062

Neuroimaging in animal models of epilepsy

Daniele Bertoglio[a,b], Jeroen Verhaeghe[b], Stefanie Dedeurwaerdere[a,1], Olli Gröhn[d*]

[a]Department of Translational Neurosciences, University of Antwerp, Wilrijk, Belgium

[b]Molecular Imaging Center Antwerp, University of Antwerp, Wilrijk, Belgium

[c]Biomedical NMR research group, Biomedical Imaging Unit, University of Eastern Finland, Kuopio, Finland

[1]Present address: UCB Pharma, Braine-l'Alleud, Belgium

*Corresponding author:

Prof. Olli Gröhn

Biomedical Imaging Unit, Department of Neurobiology,

A. I. Virtanen Institute for Molecular Sciences, University of Eastern Finland,

PO Box 1627, FI-70211 Kuopio, Finland.

E-mail: olli.grohn@uef.fi

Abstract

Epilepsy is one of the most common chronic neurological conditions worldwide. The current poor understanding and lack of reliable biomarkers of the epileptogenic process are the major limitations in the development of anti-epileptic drugs that are able to prevent or modify the underlying disease. The rapid progress in advanced imaging technologies has expanded our opportunities to study the disease in animal models of epilepsy by means of non-invasive research tools.

Here we review the advances of different *in vivo* imaging techniques, including magnetic resonance-based and nuclear imaging-based modalities, in animal models of epilepsy. Together these techniques can be applied to visualize and quantify structural, metabolic, functional and molecular changes in longitudinal study designs to provide unique information about early pathophysiological changes and their interplay involved in epileptogenesis, monitoring the disease progression, assessing the effectiveness of possible therapies, and potentially identify translatable biomarkers for clinical use.

Abbreviations

MRI = magnetic resonance imaging

PET = positron emission tomography

SPECT = single-photon emission computed tomography

NMR = nuclear magnetic resonance

RF = radio frequency

SE = status epilepticus

KA = kainic acid

TBI = traumatic brain injury

Na^{+} = sodium

ADC = apparent diffusion coefficient

ADC_{av} = averaged ADC

D_{av} = averaged diffusion constant

MD = mean diffusivity

DTI = diffusion tensor imaging

FA = fractional anisotropy

$D_{\parallel}$ = axial diffusivity

$D_{\perp}$ = radial diffusivity

DEC = directionally encoded

3D = three-dimensional

fMRI = functional MRI

BOLD = blood oxygenation level dependent

EEG = electroencephalogram

rsfMRI = resting state fMRI

MEMRI = manganese-enhanced MRI

Mn^{2+} = manganese

Ca^{2+} = calcium

BBB = blood-brain barrier

CBF = cerebral blood flow

CBV = cerebral blood volume

DCE = dynamic contrast enhanced

MTT = mean transmit time

KASE = kainic acid-induced SE

ASL = arterial spin labeling

MRS = magnetic resonance spectroscopy

^{1}H-MRS = proton MRS

NAA = N-acetyl aspartate

mIns = myo-Inositol

GSH = glutathione

GABA = gamma-aminobutyric acid

FDG = 2-fluoro-2-deoxy-D-glucose

PTZ = pentylenetetrazole

2-DG = 2-deoxy-D-glucose

SRS = spontaneous recurrent seizures

TLE = temporal lobe epilepsy

cBZ = central benzodiazepine

FMZ = flumazenil

CA = cornu ammonis

Bmax = receptor density

Kd = affinity

$D_{2/3}R$ = dopamine receptor 2 and 3

mGluR5 = metabotropic glutamate receptor 5

NMDA = N-methyl-D-aspartate

TSPO = translocator protein

P-gp = P-glycoprotein

Key Words:

MRI, PET, functional imaging, molecular imaging, epilepsy, animal model

Contents

Introduction

Small animal MRI in epilepsy research

- Anatomical MRI and relaxation-time mapping
- Diffusion MRI
- Functional MRI and resting state fMRI
- MRI with contrast agents
  - Manganese-Enhanced MRI
  - Gadolinium and iron oxide contrast MRI
- Arterial spin labeling
- Magnetic resonance spectroscopy

Small animal PET and SPECT imaging in epilepsy research

- Imaging brain activation
- Imaging brain receptors
- Imaging brain inflammation and drug resistance

Conclusion and perspectives

Acknowledgements

References

INTRODUCTION

Epilepsy is a common neurologic disease affecting more than 50 million people worldwide (WHO, 2016). It is characterized by the occurrence of spontaneous recurrent seizures and high prevalence of comorbid medical disorders, such as depression and anxiety, resulting in a devastating impact on patient's daily life (Keezer et al., 2016).

Currently, epilepsy can only be treated by anti-epileptic medication or surgery upon diagnosis. However, these anti-epileptic drugs often have adverse side-effects, are ineffective in about 30% of patients and they do not stop or interfere the underlying epileptogenic process (Shultz et al., 2014). Hence, therapies capable of preventing or halting epileptogenesis are needed. However, the lack of reliable biomarkers and the limited understanding of the epileptogenic process are the major limitations in the development and implementation of such therapies (Pitkanen et al., 2016).

The use of animal models offers the advantage to investigate different stages of epileptogenesis before the manifestation of the disease, something that is unfeasible to obtain in patients. Neuroimaging technologies are not limited to structural imaging, but molecular and functional imaging techniques allow us to investigate alterations in receptors, metabolism, and activity in the brain undergoing degenerative or plastic changes during epileptogenesis. Neuroimaging in animal models provides non-invasive tools capable to identify early biomarkers involved in epileptogenesis, longitudinally monitor disease progression, and assess effectiveness of epileptogenic therapies (Dedeurwaerdere et al., 2007; Goffin et al., 2008) .

This article focuses on *in vivo* imaging modalities, including magnetic resonance imaging (MRI), and nuclear imaging-based modalities, namely positron emission tomography (PET) and single-photon emission computed tomography (SPECT), non-invasive imaging tools that can also be used in patients. The first section reviews the application of MR approaches and the second section, PET and SPECT in animal models of epilepsy.

SMALL ANIMAL MRI IN EPILEPSY RESEARCH

MRI is based on nuclear magnetic resonance (NMR) phenomenon that can be measured when certain biologically important nuclei, such as ^{1}H, ^{13}C and ^{31}P are placed in a high magnetic field. As many of these nuclei form an essential part of the biological systems, being building blocks for water and organic molecules, MRI signal can be measured without any external tracers or radioactive irradiation. As MRI signal is in the radiofrequency (RF) part of the electromagnetic spectrum, it has excellent tissue penetration and minimal interaction with tissue which makes MRI a non-invasive and safe imaging technique.

An MR image is formed by combining RF-pulses and pulsed magnetic field gradients in time dependent manner in so-called pulse-sequence. The manipulation of the MRI signal during the pulse-sequence can be done in number of different ways leading to different MRI contrast that can be sensitized to tissue composition, microstructure, brain function, or metabolism. Furthermore, MRI has full brain coverage, excellent spatial resolution and good temporal resolution. Considering the large variety of MRI approaches currently available, MRI should be considered an armamentarium of imaging techniques instead of a single modality. Altogether, it is not surprising that MRI has been increasingly used in *in vivo* assessment of epileptogenesis and epilepsy both in animal models and in clinical settings.

MRI techniques translate extremely well from experimental settings in small animals to human studies and clinical settings. The major challenge for translation is the small size of the mice and rats, which are most often used in animal models of epilepsy. In order to achieve similar anatomical resolution as in humans, voxel size of 100-200 µm (in-plane) is needed. As acquired signal (and signal to noise ratio) is directly proportional to voxel size, high magnetic field and dedicated sensitive RF-coils have to be used in small animal MRI. Currently, strength of the main magnetic field in small animal MRI systems varies typically between 4.7 T – 11.75 T, while >20 T microimaging systems exists. Operation in high magnetic field does not come without problems: magnetic field distortions caused by different magnetic susceptibilities are higher and relaxation times are different. Therefore, techniques cannot be directly adopted from clinical MRI, however, with proper adjustment similar MRI data can in most cases be acquired both from humans and animal models. Several MRI studies have been performed in animal models of epilepsy as summarized in Appendix A.

Anatomical MRI and relaxation-time mapping

Anatomical imaging is the cornerstone of practically all MRI protocols. Basic anatomical contrast in MRI is created by different T1 and T2 relaxation times that are characteristic for different tissues or pathologies. T2 weighting is most often used to obtain an anatomic contrast in small animal MRI, while T1 weighting is typically used to achieve anatomic contrast in human imaging. This is because relaxation times are magnetic field-dependent and higher magnetic field strengths (major or equal to 4.7T) are used in small animal MRI compared to clinical MRI (1.5T – 3T).

By adjusting the timing parameters in the pulse sequence MRI can be sensitized to either T1 or T2 relaxation and corresponding image is said to be either T1 or T2 weighted. T1 and T2 relaxation times in tissue are largely determined by the amount of water, macromolecular content and presence of paramagnetic substances such as iron. Therefore, for example high grey/white matter contrast can be produced due to high myelin content in white matter, edema can be visualized because of high water content and hemorrhages are highly visible because of iron. However, it should be noted that as relaxation based contrast is sensitive to number of different changes in tissue it is not very specific, and interpretation of signal intensity changes in T1 or T2 weighted images is often ambiguous.

Apart from sufficient image contrast between the tissue types, another requirement for anatomical imaging is high enough spatial resolution compared to size of the area of interest. The typical in-plane spatial resolution easily achievable with a dedicated small animal MRI system is on the order of 100 μm^2, while slice thickness is typically larger, on the order of 0.5-1.0 mm. Increasing the measurement time and using advanced hardware such as a very high magnetic field (≥ 9.4T) and/or cryogenic RF-coils, can lead to an isotropic resolution in the order of 50-100 μm^3 (Baltes et al., 2009), which provides excellent separation of many anatomic structures of interest for epilepsy studies. However, for very high resolution scanning time ranges between 0.5 and 2 hours and achieving the similar anatomical resolution in clinical settings is currently very difficult due to technical limitations and the introduction of motion artifacts by the subject.

In epilepsy models, anatomic T1- or T2-weighted imaging is usually used to detect initial edema or microhemorrhages caused by status epilepticus (SE), or other epileptogenic brain

insults or tissue atrophy. In SE models (e.g., systemic injection of kainic acid (KA) or pilocarpine), the typical finding is high signal intensity on T2-weighted images in the amygdala and the piriform and entorhinal cortices beginning 2 h after SE, and peaking 12-24 h after SE (Roch et al., 2002b; Fabene et al., 2003; Fabene et al., 2006), followed by normalization of the contrast over subsequent days and weeks (Roch et al., 2002a) when the water has been reabsorbed from the edematous lesion. Progressive development of atrophy can be seen as an increase in the ventricle size, a decrease in the size of the hippocampus, and cortical thinning within weeks to months after SE (Wolf et al., 2002; Nairismagi et al., 2004; Polli et al., 2014). Similar changes (acute edema – reabsorption – atrophy) with a delayed time-course can be observed with other brain damaging epileptogenic insults such as stroke or traumatic brain injury (TBI), in which hemorrhage from microbleeds is also often detected (Immonen et al., 2009a). In addition, structural atrophy has been reported to relate with functional performances (Niessen et al., 2005; Immonen et al., 2009b).

T1 and T2 relaxation times are physical quantities that can be reproducibly quantified. Therefore, progression of pathology can be also followed by quantitative mapping of relaxation times rather than signal intensity in T2- or T1-weighted images (Bouilleret et al., 2000; Nairismagi et al., 2004). Relaxation times are magnetic field dependent and to certain extend they depend on pulse sequence parameters. Still, with proper harmonization, relaxation times can provide comparable absolute values between laboratories, and therefore have high value as potential biomarkers of tissue damage in the context of epileptogenesis. Indeed, recent work demonstrated an excellent predictive value of $T_{1\rho}$ relaxation time (rotating frame variant of T1 relaxation) measured in the perilesional cortex after TBI in rats for increased seizure susceptibility (Immonen et al., 2013). Also, after hyperthermia-induced SE in the rat on postnatal day 11, reduced T2 relaxation time in the amygdala, likely associated with deoxygenated blood, was a prognostic biomarker for epileptogenesis (Choy et al., 2014). In addition, T2 relaxation time in the amygdala in rats 30 days following pilocarpine-induced SE correlated with hyperactivity behavior during open field test (Suleymanova et al., 2016). Finally, Dietrich and colleagues reported correlations between T2 relaxation time with the number and duration of hippocampal paroxysmal discharges measured during epileptogenesis in the intrahippocampal KA mouse model of epilepsy (Dietrich et al., 2016).

Diffusion MRI

Amount and direction of self-diffusion of water can be utilized as MRI contrast. Diffusion of water is restricted by cellular structures such as myelin sheets and cell membranes, and therefore water diffusion relays information about the microstructure of the tissue and water distribution within different cellular compartments.

The most commonly used diffusion MRI parameter is the apparent diffusion coefficient (ADC), which gives the magnitude of the restricted diffusion and can be either orientation-invariant or orientation-dependent. In the early diffusion work, diffusion sensitizing gradients were often applied in only one physical direction, giving ADC values that are sensitive not only to the magnitude of the diffusion but also to the orientation of the structures, while more recent studies have exploited almost entirely orientation-invariant approaches, and corresponding diffusion metrics is called averaged ADC (ADC_{av}), averaged diffusion constant (D_{av}), mean diffusivity (MD), or diffusion trace (more accurately 1/3 of the trace of the diffusion tensor).

After brain insults leading to epilepsy, the ADC can be either decreased or increased. During the first hours after insult, a rapid diffusion drop down to about 60-80% of normal value can be detected. This initial diffusion drop has been detected both in status epilepticus and focal lesion models including traumatic brain injury and stroke (Zhong et al., 1993; Kharatishvili et al., 2007). Initial diffusion decrease is associated with so-called cytotoxic edema and it has been best characterized in acute stroke (Moseley et al., 1990). Cytotoxic edema is defined as a condition where energy failure in the tissue leads to the inability of cells to maintain a high extracellular and low intracellular sodium (Na^+) concentration. This is followed by osmolarity-driven water shifts from the extracellular to the intracellular space, leading to cell swelling without a net increase in the tissue water content. This acute ADC decrease is followed by gradual increase of ADC when cytotoxic edema is resolved and cellular structures start to degrade leading first to pseudo normalization within a day or few days, and to increased ADC on mature lesion after several weeks to months. When biphasic temporal profile of ADC changes is combined with typical temporal profile of relaxation time changes, the severitity of the initial damage and progression of lesion can be estimated

(Nairismagi et al., 2004; Grohn et al., 2011) and potentially used as biomarker for hyperexcitability and epilepsy. Indeed, it was recently shown that ADC changes in hippocampus both in acute and in chronic time-points correlated with chronic hyperexcitability in fluid percussion post-traumatic epilepsy model (Kharatishvili et al., 2007). Similar finding was obtained in the pilocarpine mouse model of epilepsy (Kharatishvili et al., 2014). Furthermore, in a recent study using hippocampal electrical stimulation model specific T2 and diffusion changes were observed only in rats that developed spontaneous limbic seizures (Parekh et al., 2010).

Diffusion MRI can also measure orientation of the tissue restricting structures when it is measured in at least six orthogonal directions. The anisotropy of the diffusion (diffusion tensor) is the basis for diffusion tensor imaging (DTI), which can be used to detect microstructural changes caused by epileptogenic insults. The simplest and most often used parameter derived from diffusion tensor is fractional anisotropy (FA) which indicates how much diffusion behavior deviates from isotropic diffusion. Other commonly used scalar DTI metrics include axial and radial diffusivity (D_{II}, $D_{\perp}$), giving the average amount of diffusion in the principle diffusion direction and perpendicular to that, respectively.

FA, D_{II}, and $D_{\perp}$ are used to characterize white matter changes in many epilepsy models. Decrease in FA is often used as a nonspecific marker related to the degradation of oriented structures, while changes in D_{II} have been explained by axonal damage and an increase in $D_{\perp}$ by demyelination (Song et al., 2002). Even though this relatively widely spread view can be used as a good starting point in interpretation of DTI results, there is growing awarness that multiple factors may affect all commonly used scalar DTI metrics. Recently, DTI was applied to visualize differences in white matter during chronic epilepsy between epileptic rats with distinctive seizure susceptibility (Sharma et al., 2017). Furthermore, DTI in combination with contrast agent MRI (see below) has also been used to determine both microstructural and diffusion changes during ictal state (Mizoguchi et al., 2017) and postictal state (Hamamoto et al., 2017) in cats with familial spontaneous epilepsy.

Very high-resolution DTI has been used to characterize layer-specific changes in the hippocampus after various epileptogenic brain insults (Sierra et al., 2015). Interestingly, increased FA in the rat dentate gyrus several months after SE is associated with mossy fiber sprouting and reorganization of axons in the outer molecular layer, indicating that DTI has the potential to visualize structural plasticity at the axonal level during epileptogenesis (Kuo

et al., 2008; Laitinen et al., 2010; Sierra et al., 2015) (Fig. 1) as well as chronic effects of seizures during early development (Sayin et al., 2015). Furthermore, astrocyte processes may significantly contribute to orientation of water diffusion in epileptogenic hippocampus (Salo et al., 2017). It should be noted, that these very high-resolution approaches require typically very long scanning time making translation of the results to human studies challenging.

Combining orientation information from multiple voxels in three-dimensional (3D) MRI data allows for tracing of white matter tracts. The modern DTI tractography approaches rely on data acquisition and reconstruction strategies that go beyond classical DTI and can also separate crossing fiber populations. The use of tractography in animal studies is much more limited than in human studies due to technical difficulties in obtaining high-resolution 3D data with sufficient resolution to reliably resolve white matter tracts. Another issue is directionality, which may be anterograde or retrograde as we are observing motion of water molecules, and it cannot be differentiated in axons (Mori and Zhang, 2006). In spite of these limitations the feasibility of tractography in small animals has been demonstrated (Kim et al., 2012), however, it has not yet been widely applied to animal models of epilepsy. Overall, this approach holds great promise for assessing the network level reorganization associated with epilepsy, especially when used together with functional connectivity analysis (see below).

Functional MRI and resting state fMRI

Functional MRI (fMRI) measures brain activity indirectly through hemodynamic changes that are associated with brain activity through neurovascular coupling. Neurovascular coupling model states that there is a functional hyperemia in the short vicinity (200-250 µm) of the activated brain area. This hyperemia overcompensates increased oxygen consumption in the activated area leading excess amount of deoxyhemoglobin. As deoxyhemoglobin is paramagnetic and oxyhemoglobin diamagnetic, T2 and $T2^*$ relaxation time increases in the activated brain area. This can be measured by so-called blood oxygenation level dependent (BOLD) contrast, which is the most common approach for fMRI (Jonckers et al., 2015). As BOLD fMRI response is result of complex cascade relying neuronal activation to

hemodynamic response, fMRI experiment in epileptic animals requires careful control of the animal physiology and an understanding of the effects of anesthesia on basal blood flow level, neurovascular coupling, and seizures.

Classical way of doing fMRI is to use a stimulation protocol with known resting and activation periods. In data analysis, signal intensity in acquired BOLD time series is statistically compared with expected signal time course obtained by convoluting stimulation paradigm with hemodynamic response function. Therefore, time when brain activation takes place is required as a starting point in most fMRI data analysis approaches, although data-driven approaches also exist. In epilepsy models, the timing information of the abnormal brain activity can be obtained from simultaneously recorded electroencephalogram (EEG) or local field potential data. Even though simultaneous fMRI/EEG is a demanding technique, especially in high magnetic field used in small animal MRI, it is feasible and has been applied to study spatiotemporal progression of both spontaneous and induced seizures in various animal models (Blumenfeld, 2007; Englot et al., 2009; Motelow et al., 2015; Cleeren et al., 2016). Furthermore, fMRI/EEG has been used to investigate involvement of the different brain regions and networks on spike-wave seizures in WAG/Rij rats and impaired consciousness during the seizures (Englot et al., 2009; Motelow et al., 2015).

Resting state fMRI (rsfMRI) measures the temporal variation of the fMRI signal without an external stimulus or presence of seizure activity. When the resting-state fMRI signal timecourses correlate between two brain regions, the brain regions are considered to be functionally connected. As epilepsy is increasingly recognized to be a network-level disease, this kind of approach has a great promise for detecting large scale network level alterations in epileptogenic brain. Resting-state analyses are increasingly used in human epilepsy studies, and are also feasible in rodents (Gozzi and Schwarz, 2016). In a recent study, rats with increased seizure susceptibility following lateral fluid percussion injury, a traumatic brain injury model, were used (Mishra et al., 2014). The group statistics revealed decreased connectivity between the ipsilateral and contralateral parietal cortex and between the parietal cortex and hippocampus on the side of injury as compared to sham-operated animals. Injured animals also had abnormal negative connectivity between the ipsilateral and contralateral parietal cortex and other regions. Another work utilized graph theory analysis of functional connectivity data in a rat model of mild facial seziures caused by injection of tetanus toxin into the right primary motor cortex. The results indicated that,

despite the locality of the epileptogenic area, epileptic brains exhibit a different global network topology, connectivity, and structural integrity than healthy brains (Otte et al., 2012). Consistently, a recent study investigated the graph topological properties of brain networks during chronic epilepsy in KASE rats. The authors reported extensive disruptions in the functional brain networks of epileptic rats compared to control animals (Gill et al., 2017). While longitudinal studies have been challenging, especially when combining EEG and fMRI, recent work demonstrated both EEG and resting state connectivity changes after status epilepticus utilizing implatable RF-coil and electrodes (Fig. 2) (Pirttimaki et al., 2016).

MRI with contrast agents

Manganese-enhanced MRI

Inherent properties of manganese (Mn^{2+}) ion make possible different manganese-enhanced MRI (MEMRI) approaches in animal models (Silva et al., 2004). Mn^{2+} is paramagnetic, and as it shortens T1 relaxation time it can be detected by conventional T1 imaging. What makes Mn^{2+} interesting as a contrast agent is that it has approximately the same radius and charge as calcium (Ca^{2+}) acting as a Ca^{2+} analogue in the brain. It accumulates into cells as it can enter cells through Ca^{2+}-channels and is stored in Ca^{2+} storing organelles and vesicles. Part of the Mn^{2+} accumulation depends on activity of Ca^{2+}-channels and Mn^{2+} is also transported in axons similarly to Ca^{2+}. Therefore, MEMRI can be utilized as structural, functional, and tract-tracing contrast agent, thus highlighting different aspects of epileptogenic processes and epilepsy.

Unique structural contrast can be achieved by systemic Mn^{2+} injection as Mn^{2+} does not accumulate evenly in all cell types. This allows for example visualization of cortical layers and hippocampal subfields in normal brain (Silva et al., 2008). Multiple factors influence the accumulation speed and final concentration of Mn^{2+} in the tissue including blood-brain barrier (BBB) permeability, basal functional activity and Ca^{2+} storing capacity of cells. MEMRI after systemic injection has been applied to several different animal models of epilepsy and variable results have been obtained depending on type of the model, and time-point after induction of epileptogenesis. This could be related to a possible confounding effect of manganese as contrast agent given its toxicity with long-term structural and functional consequences (Bouilleret et al., 2011). Toxicity severely limits its clinical application and

represents the major drawback of this technique (Malheiros et al., 2015). Indeed, chronic exposure to Mn^{2+} leads to manganism, a progressive neurodegenerative condition similar to Parkinson's Disease (Mena et al., 1967), while the exposure to manganese following acute systemic administration of contrast agent, may result in hepatic failure, cardiac toxicity, and death (O'Neal and Zheng, 2015).

MEMRI changes in epilepsy models have been associated with glial cells, mossy fiber sprouting, BBB leakage and altered brain activity (Nairismagi et al., 2006; Alvestad et al., 2007; Hsu et al., 2007; Immonen et al., 2008; Dedeurwaerdere et al., 2013). This diversity is understandable considering the mechanism behind Mn^{2+} accumulation and complexity of the pathophysiology of epileptogenesis and epilepsy.

MEMRI can be used also as functional imaging approach, as Mn^{2+} enters cells through activity dependent calcium channels. In most brain areas, penetration of Mn^{2+} through BBB is the rate-limiting step for Mn^{2+} accumulation. For example, SE induced by either kainic acid or pilocarpine injection does not lead to increased hippocampal MEMRI contrast despite high cellular activity (Immonen et al., 2008; Malheiros et al., 2014). Therefore, in functional MEMRI studies BBB permeability is typically increased by administering mannitol. Recent studies demonstrated that activity-dependent accumulation of Mn^{2+} in the brain can also be detected with an intact BBB, but this appears to be brain region-dependent and may require extended Mn^{2+} administration by subcutaneous mini pump approach (Eschenko et al., 2010), which may open interesting new study designs also for experimental epilepsy studies.

MEMRI can be used also for *in vivo* track tracing after intracranial injection as Mn^{2+} is actively transported in axons, similar to Ca^{2+}. This approach was exploited to specifically label a certain cell population in hippocampus (Nairismagi et al., 2006). Mn^{2+} was injected into the entorhinal cortex, from which it was transported via the perforant pathway to granule cells in the hippocampus leading to specific labeling of the mossy fiber pathway. This approach allowed visualization of mossy fiber sprouting, which is one of the hallmark features in temporal lobe epilepsy, three weeks after induction of SE, and highlights unique ability of MEMRI to detect cell-specific plasticity during epileptogenesis in the brain.

Gadolinium and iron oxide contrast MRI

Gadolinium and superparamagnetic iron oxide based contrast agents are often used to measure hemodynamic parameters (cerebral blood flow (CBF) or cerebral blood volume (CBV)) and blood brain barrier integrity in epilepsy models. Gadolinium is most often detected through a T1 shortening effect, while superparamagnetic iron oxide contrast agents provide very strong T2 and T2* contrast. Gadolinium has been commonly thought to be risk-free, however, recent clinical studies revealed higher risk of nephrogenic systemic fibrosis (risk of 2.4% per gadolinium exposure (Deo et al., 2007)), which can cause systemic fibrosis and even death (Penfield and Reilly, 2007), limiting its application in patients. In addition, gadolinium administration causes acute kidney injury, which advises extreme caution when considering patients with renal dysfunction (Penfield and Reilly, 2007).

CBF and CBV mapping can be performed using a dynamic contrast enhanced (DCE, also called bolus tracking) approach, which is comparable to DCE methods used in clinical settings. In this approach, signal intensity changes during first pass bolus of contrast agent can be measured using rapid imaging sequences with temporal resolution of 0.5-1 s. Relative CBV, CBF and mean transmit time (MTT) can be calculated after fitting the data to gamma variate function. Another approach is to use intravascular contrast agents, typically superparamagnetic T2/T2* contrast agents. As this kind of contrast agents stay in the intravascular space for extended period, signal intensity difference before and after contrast agent injection reflects the amount of blood in the imaging voxel. As there is no need to follow dynamics of the contrast agent induced changes, more time can be used for imaging and high resolution CBV maps can be obtained. An example of hemodynamic imaging in status epilepticus model, shows increased CBF and CBV in amygdala. This was associated with increased vessel density, indicating that epileptogenesis may involve hemodynamic changes that are associated with vascular reorganization during post-SE remodeling (Hayward et al., 2010).

Contrast agents remain mainly inside blood vessels in the healthy brain with an intact BBB. Therefore the leakage of the contrast agent outside the vessels can be used as a marker of damaged BBB. As BBB damage has been recognized to play a role in epileptogenesis, imaging of BBB has attracted increasing amount of attention in the epilepsy field. In the conventional approach T1-weighted images are measured before and after gadolinium-bolus injection. A recent improvement of the technique that incorporates step-down infusion of gadolinium instead of bolus injection and quantitative relaxation mapping can detect markedly more

subtle BBB damage and has indeed been shown to detect BBB damage in specific brain regions for up to 6 weeks after kainic acid-induced SE (KASE) in rat (van Vliet et al., 2014). Interestingly, the same approach was recently used as biomarker for monitoring the effect of rapamycin treatment in a rat SE model (van Vliet et al., 2016) as well as to evaluate the efficacy of isoflurane treatment during induction of SE on BBB impairment 2 days after SE (Bar-Klein et al., 2016). In addition, Breuer and colleagues reported higher sensitivity of gadolinium-enhanced T1-weighted MRI compared to ^{68}Ga-DTPA PET and ^{99m}Tc-DTPA SPECT in detecting BBB impairment following SE in rats (Breuer et al., 2017). Another approach recently described involves the employment of iron-filled nanoparticles as contrast agent to monitor brain distribution of iron-labeled transplanted bone marrow stem cells in rats (Long et al., 2015) or brain uptake by myeloid cells in pilocarpine SE-induced mice (Portnoy et al., 2016).

Arterial spin labeling

CBF can also be measured without an external contrast agent using arterial spin labeling (ASL). In this technique, RF-pulses are used to label inflowing blood by saturating or labeling the inflowing blood, typically at the level of the neck. Control image with non-labeling RF-pulse is subtracted from the labeled image and the small difference in signal intensity caused by the inflow of the magnetically labeled blood is proportional to the blood flow. The advantage of this approach is that CBF can be quantified in absolute units, and follow-up studies do not require repetitive cannulation and administration of contrast agents but the approach has an inherently lower contrast-to-noise ratio and thus requires a longer acquisition time than the CDE approach with contrast agent. ASL has been used to assess contribution of insufficient blood flow to hippocampal damage caused by pilocarpine induced seizures in rat (Choy et al., 2010), to investigate changes during KASE in rats (Sakurai et al., 2015), and for longitudinal characterization of CBF changes in post-traumatic epilepsy model (Hayward et al., 2011).

Magnetic resonance spectroscopy

As MRI is basically just another NMR technique, it can be used to analyze chemical composition of tissue in the similar manner as NMR spectroscopy is used to analyze chemical

composition in a test tube. In the context of *in vivo* imaging, this approach is called magnetic resonance spectroscopy (MRS). In practice, only signal coming from small molecules in tissue with long enough T2 relaxation time can be measured, limiting the use of *in vivo* proton (^{1}H-) MRS for detection of approximately 20-30 metabolites, which are present with high enough (mM) concentration, in the brain. As ^{1}H-MRS detects small metabolite signal in the presence of much higher water or fat signal, even relatively small methodological imperfections may lead severely compromised quality of ^{1}H-MR spectra and large errors in quantification of the metabolite concentration. Therefore, it is essential that experts who understand the requirements for sensitivity of RF-coils, magnetic field shimming, and details of pulse sequence (including water suppression, outer volume suppression, pulse bandwidths, and similar) will participate in implementation of the method.

In spite of technical challenges, ^{1}H-MRS has been actively used in combination with epilepsy models. This is as several metabolites detectable by ^{1}H-MRS contain complementary information about processes that have been associated with epileptogenesis or epilepsy both in animal and in human brains. N-acetyl aspartate (NAA) is present mostly in neurons and is considered marker of neuronal viability (Rigotti et al., 2007). While acute NAA changes may occur after status epilepticus before neuronal death (Ebisu et al., 1996) and can be reversible, NAA decrease in chronic phase is associated with neuronal injury (Simister et al., 2002) and has been used in lateralization in humans. Accordingly, a decrease in NAA was reported in status epilepticus rat models during acute stage (Tokumitsu et al., 1997; van Eijsden et al., 2004; Gomes et al., 2007; Filibian et al., 2012; Lee et al., 2012; Wu et al., 2015) as well as chronic phase of disease (Tokumitsu et al., 1997; Filibian et al., 2012; Lee et al., 2012). Lactate is elevated in tissue during and after seizures as a consequence of compromised energy homeostasis. Myo-Inositol (mIns) participates osmoregulation in the brain. It is often considered as metabolic marker for glial cells and is found to be elevated in several animal models before onset of spontaneous seizures, and during epilepsy. As glial cell activation has been recently recognized to play an important role in epileptogenesis, quantitation of mIns by *in vivo* MRS may provide a biomarker for epileptogenesis (Vezzani et al., 2017). An increase in mIns levels during epileptogenesis in SE models has been reported (Filibian et al., 2012; Lee et al., 2012). In addition, Filibian and colleagues found that mIns and glutathione (GSH) increases negatively correlate with the extent of neurodegeneration in the hippocampus (Filibian et al., 2012). This was supported by a recent study in a

pilocarpine status epilepticus model in 21-day old rats, where 60–70% of animals develop spontaneous seizures after around 70 days. Notably, authors found that increased mIns levels before the onset of epilepsy could predict with high accuracy which animals develop the disease (Pascente et al., 2016). Additionally, Van der Hel and colleagues reported a reduction in gamma-aminobutyric acid (GABA) and glutamate in the same status epilepticus model before the onset of spontaneous seizures (van der Hel et al., 2013). A recent study showed that sodium selenate treatment prevents changes in NAA or mIns in a rat SE epilepsy model suggesting a protective effect during epileptogenesis (Liu et al., 2016). Finally, Pearce and colleagues segregated KASE rats in two distinctive clusters based on differences in metabolic parameters in the dentate gyrus 3 days post-SE, which persisted 3 weeks following status epilepticus according to injury severity (Pearce et al., 2016).

In addition to ^{1}H-MRS, ^{31}P- and ^{13}C-MRS can provide information, for example, about energy and glucose metabolism, however, the utilization of these nuclei is somewhat limited due to inherently low signal leading to impractically large voxel size for some applications. So far, one study investigated the effect of a single injection of KA on astrocytic and neuronal metabolism in mice by means of ^{13}C-MRS using 13C labeled metabolic substrates ([1,2-^{13}C]-acetate and [1-^{13}C]-glucose) (Walls et al., 2014).

SMALL ANIMAL PET AND SPECT IMAGING IN EPILEPSY RESEARCH

The potential usefulness of small animal PET was first conceptualized in the late-90s (Hume and Jones, 1998). The introduction of dedicated high-resolution small animal PET and SPECT cameras has made it possible to visualize and quantify functional processes in the brain of rodents. PET and SPECT imaging is based on the use of radiotracers, i.e. biological relevant molecules labeled with a radioactive isotope, that is administered to the animal and will accumulate throughout the body in a tracer dependent fashion. PET imaging uses positron emitting isotopes, the emitted positrons in turn will annihilate with nearby (≈ 1mm) electrons resulting in the emission of two high-energy anti-parallel gamma rays. The coincidences (i.e., simultaneously detected photons 180° apart) are detected by a ring of photosensitive crystals and subsequently, these lines of coincidence are reconstructed into a

3D image (Phelps, 2000). SPECT, on the other hand, uses isotopes that emit a single photon or gamma ray that is detected by physical collimation (allowing only rays in a certain direction to reach the detector) followed by capturing of the gamma ray by the detector (Phelps, 2000).

A clinical limitation of these techniques is the sensitivity to movements of the patient's head during the acquisition since it might hamper the interpretation of the images (Salmon et al., 2015). However, different methods are available to correct head movements during the acquisition (Montgomery et al., 2006). Furthermore, PET and SPECT imaging involve exposure to ionizing radiation, which dosimetry may limit the translation of radioligands into clinic.

Nevertheless, PET and SPECT imaging provide a powerful experimental approach to investigate the nature and evolution of brain changes occurring over time in the different animal models of epilepsy. Several radiotracers have been used in experimental epilepsy research to visualize and quantify changes in brain activation, receptor density, and brain inflammation as summarized in Appendix B.

Imaging brain activation

The focus of several nuclear imaging studies in models of epilepsy was to investigate alterations in brain glucose metabolism with 2-[^{18}F]fluoro-2-deoxy-D-glucose ([^{18}F]FDG), a glucose analogue labeled with the positron emitter ^{18}F , as previously discussed (O'Brien and Jupp, 2009; Mirrione and Tsirka, 2011). A strong increase in brain glucose metabolism is observed following acute seizures provoked by excitotoxins such as kainic acid and pilocarpine in rats and mice with FDG small animal PET (Kornblum et al., 2000; Mirrione et al., 2006; Mirrione et al., 2007). Studying glucose metabolism or blood flow with PET and SPECT may help to elucidate the mechanisms of seizure generation. For instance, Mirrione and colleagues demonstrated that FDG uptake following pilocarpine administration differed between transgenic tissue plasminogen activator knockout mice and WT animals (Mirrione et al., 2007).

Kindling allows for the timed investigation of seizure generation and propagation during the process of epileptogenesis. Autoradiographic studies revealed that a large number of cortical

regions are involved already at the first kindling stages (Chassagnon et al., 2006). Recently, Bascunana and colleagues have shown that FDG-PET can be employed to differentiate between animals resistant and non-resistant to pentylenetetrazole (PTZ) kindling, with the kindled animals (non-resistant) characterized by hypometabolism (Bascunana et al., 2016).

In a study using ^{99m}Tc-ECD SPECT, two rhesus monkeys followed longitudinally exhibited different spatial patterns of blood perfusion clustering over time (Cleeren et al., 2015); a first perfusion cluster showing hyperperfusion that expanded during the kindling procedure (likely to represent the epileptogenic network), a second type showing hypoperfusion initially but then hyperperfusion in the later phases, and the third cluster showing hypoperfusion that expanded during the kindling process. As temporal resolution is a limitation of this technique, as a consequence the start, middle, end or combinations of the different seizure phases are measured, depending on when perfusion ligand is injected, which may introduce additional variability.

Several studies took advantage of the strength of non-invasive small animal PET by imaging interictal alterations during epileptogenesis (Goffin et al., 2009; Guo et al., 2009; Jupp et al., 2012; Lee et al., 2012)**.** In post-SE rat models, brain glucose hypometabolism occurs early (within 1-2 days) in the processes of limbic epileptogenesis and mirrors the areas with strong hypermetabolism during SE. The widespread hypometabolism normalizes for most of the extra-temporal regions in the chronic epilepsy phase, but can persist in limbic structures such as the hippocampus and temporal lobe (Goffin et al., 2009; Guo et al., 2009). This was confirmed by other studies (Jupp et al., 2012; Lee et al., 2012) and has also been observed in 2-deoxy-D-glucose (2-DG) autoradiography studies (Nehlig and Obenaus, 2006). For the first time, imaging studies made it possible to investigate the link between early hypometabolism and the development of epilepsy. Interestingly, Guo and colleagues found that early (day 2) hypometabolism in the entorhinal cortex correlated with later development of spontaneous recurrent seizures (SRS) monitored by continuous EEG recordings over 6 weeks (Guo et al., 2009). More specifically, early FDG uptake was positively correlated with the duration of the latent phase (R^2 = 0.781) as well as with the frequency of the SRS (R^2 = -0.907) during the chronic period. These exciting findings still require further confirmation. The study by Jupp et al. (2012) could not investigate this relation, as they did not perform continuous EEG monitoring (Jupp et al., 2012), but Goffin and colleagues, using continuous video-EEG

monitoring, reported that 3 of the 7 animals developed seizures (Goffin et al., 2009). Intriguingly, the SRS group showed less severe early (day 3) hypometabolism (i.e., higher FDG uptake) in the striatum and hippocampus compared to the non-SRS group. The discrepancy with Guo's study is difficult to explain, but it is impossible to draw profound group-based conclusions because only small samples sizes were available. The choice of injectable anaesthesia at the time of FDG administration in the Goffin study might also have confounded the results as pentobarbital induces a general decrease in the FDG signal and may have interfered differentially with the FDG uptake. In the lateral fluid percussion injury model, a traumatic brain injury model, obvious structural differences or large alterations in FDG metabolism were not observed between SRS and non-SRS animals. More advanced analysis of the data, however, revealed subtle hippocampal surface differences between the groups. In addition, multivariate logistic regression of longitudinal FDG uptake in the ipsilateral hippocampus predicted the epilepsy outcome when different time-points were taken into account (Shultz et al., 2013). Hippocampal hypometabolism, however, did not correlate with seizure frequency based on a single time-point. Nevertheless, these data provide additional support that FDG-PET could potentially be a biomarker of epilepsy outcome following brain damage. A recent study in a traumatic brain injury mouse model investigated long-term changes in CBF as a proxy for neural activity. The authors associated the chronic increased CBF and the behavioral alterations as long-lasting consequences of TBI.

During chronic epilepsy, hypometabolism is retained or normalizes again. In the study by Guo et al. (2009), the thalamus was more affected by hypometabolism in the epilepsy group compared to the non-epilepsy group (Guo et al., 2009). Interestingly, alterations beyond the epileptogenic zone are observed and thus abnormalities in the entire brain network are now under study. There is a paradigm shift that not only is the onset zone involved in the pathophysiology of focal epilepsy, but the network recruited to propagate the seizures may also be altered. This was investigated by Choi et al. (2014a) in the chronic epilepsy phase (4-6 weeks after SE) of the pilocarpine-induced SE model based on multiscale network analysis. Interictal FDG-PET showed not only hypometabolism in several regions but also reduced connectivity (indicated by reduced interregional correlation) in the left amygdala and left entorhinal cortex (Fig. 3). Also, graph and multiscale framework analyses suggest the

presence of an abnormal left limbic-paralimbic-neocortical network. The abnormalities in the brain network partially overlap with hypometabolic areas. It seems, however, that the network-based approach also detects disrupted interregional areas such as the left amygdala where decreased FDG uptake was not observed. Still, the term “connectivity” should not be taken literally as network analysis based on interregional correlation does not provide evidence for a connection between the regions, but rather gives an idea how brain areas relate to each other within the brain network. In addition, the correlations are performed on a group level, so it is not possible to determine individual abnormalities in network properties. The asymmetric nature of these changes is interesting as brain damage is thought to be very much symmetric in systemically induced SE models. It will be interesting to see how these network changes evolve over time and to link this with the development of epilepsy and seizure burden.

Does FDG hypometabolism merely reflect cell loss? As glucose metabolism is higher in neuronal high-density areas, a contribution from cell loss to the hypometabolic signal is to be expected (Zhang et al., 2015). The findings from many clinical and preclinical studies, however, do not support a direct relation between cell loss and interictal hypometabolism in chronic epilepsy (Henry, 1996; Jupp et al., 2012; Zhang et al., 2015). Often, the extent of hypometabolism goes beyond the lesion area (Engel et al., 1982; Dube et al., 2001), which may be a consequence of reduced glucose metabolism from input regions, such as the hippocampus. In some regions, such as the hilus, cell loss has been observed without congruent hypometabolism in the pilocarpine SE model (Dube et al., 2001).

The observed hypometabolism may represent cellular potentially homeostatic mechanisms occurring early during epileptogenesis (Jupp et al., 2012). Others suggest that decreased and dysregulated activity in extra-temporal regions, particularly the thalamus, lead to increased cortical inactivity and maintenance of seizure activity (Dlugos et al., 1999; Dube et al., 2001). Whether hypometabolism immediately after SE or trauma reflects the same processes as during the chronic phase, however, remains unclear. Is hypometabolism a cause or effect of epilepsy? Can we dissect the different factors that may result in glucose metabolism alterations, such as an acute response to SE, response to brain damage, epileptogenesis, and effects of recurrent seizures? A limitation of the commonly used SE models is that these factors are cumulative. Therefore, data derived from other models may be complementary and help to increase our understanding.

The effect of several experimental therapies for epilepsy on glucose metabolism and blood flow has been tested to investigate mechanisms of action. The first study in 2005, evaluated the effect of acute and subchronic vagus nerve stimulation on FDG uptake in healthy rats (Dedeurwaerdere et al., 2005). Acute vagus nerve stimulation decreased left hippocampal FDG uptake, a brain region that is hypermetabolic during limbic seizures. After subchronic vagus nerve stimulation, there may be some level of adaptation as significant hippocampal changes were no longer observed, but this may have also been an issue of statistical power. On the other hand, subchronic vagus nerve stimulation induced alterations in the striatum, which is known to play a role in seizure control. The olfactory bulb was also identified as a region of altered FDG uptake, consistent with the existence of a vagus nerve-olfactory bulb pathway. This pilot study included only small numbers of animals and the resolution of the PET camera at that time was still low. Nevertheless, it shows the feasibility of obtaining regional information about the action of new treatments using FDG PET in small animals. More recent studies investigated the effects of deep brain stimulation (Gao et al., 2009; Wyckhuys et al., 2010), low-frequency stimulation (Wang et al., 2014) and transcranial magnetic stimulation (Wyckhuys et al., 2013) on FDG-PET or CBF with SPECT in rats to test different stimulation parameters and paradigms. In addition, several pharmacological studies aimed to prevent or reverse hypometabolism following SE using FDG PET as readout for treatment efficacy. Shiha and colleagues showed that subacute treatment with fluoxetine, a selective serotonin reuptake inhibitor, prevented short-term hypometabolism following pilocarpine-induced SE in rats (Shiha et al., 2015). Similar approach was used to evaluate the efficacy of *p*-chlorophenylalanine, a specific tryptophan hydroxylase inhibitor, without any effect (Garcia-Garcia et al., 2016). On the contrary, treatment with metyrapone, an 11β-hydroxylase inhibitor, prevented hypometabolism and brain damage caused by SE in rats (Garcia-Garcia et al., 2017).

Imaging brain receptors

As the mechanisms underlying seizures are typically attributed to an altered balance between inhibition and excitation, a decrease in inhibitory GABA neurotransmission in the hippocampus is proposed to play an important role in temporal lobe epilepsy (TLE).

Malfunctioning of GABAergic neurotransmission may be caused by several factors at the level of GABA synthesis, turnover, and release, or at the receptor itself. The latter may include loss of GABAergic interneurons, loss of $GABA_A$ receptors, or changes to $GABA_A$ receptor subunits leading to alterations in receptor properties. Imaging of the $GABA_A$ receptor may improve our understanding of this complex process. The $GABA_A$ receptor is a post-synaptic pentameric ligand-gated chloride channel with binding sites for several ligands. The central benzodiazepine (cBZ) binding site is composed of $alpha_1$ and $gamma_2$ subunits, and can be imaged with ^{11}C- or ^{18}F-labeled flumazenil (FMZ) for PET or ^{123}I-Iomazenil for SPECT (Katsifis and Kassiou, 2004).

Given the relatively low spatial resolution of PET and SPECT cameras, tracer binding can also be investigated by *in vitro* autoradiography, a technique that offers high resolution molecular imaging and allows to investigate different hippocampal layers. A detailed cross-sectional study with ^{3}H-flumazenil autoradiography during epileptogenesis in the kindling model demonstrated lamina-specific changes in receptor density (Liu et al., 2009). The receptor density in the stratum moleculare and granulosum of the dentate gyrus was increased, while it was decreased in the stratum radiatum of cornu ammonis (CA) 3 and CA2. The increase in the dentate gyrus was first observed in the stratum moleculare after 2 weeks of twice-daily kindling (range 1-4 class V seizures) and was proposed to reflect a compensatory response to hyperexcitation. In CA3 and CA2, on the other hand, decreases were restricted to the 2-week kindling time-point and normalized afterwards, while increased receptor density persisted in several areas. A subsequent study in the KASE model also demonstrated time-dependent and sub-regional hippocampal changes in $GABA_A$/cBZ receptor density (Vivash et al., 2011). While $GABA_A$/cBZ receptors are thought to rapidly internalize during SE as an explanation for the reduced efficacy of benzodiazepines (Jones-Davis and Macdonald, 2003), an initial increase was observed 24 h after SE in several hippocampal sub-layers (Vivash et al., 2011). Although in contrast with previous studies (Rocha and Ondarza-Rovira, 1999), this increase may represent a delayed transient compensatory mechanism in response to excessive excitation during SE, which could be more obvious compared to kindling due to the stronger excitotoxic insult. This was followed by a persistent decrease 2–6 weeks after SE in most hippocampal regions, except for the stratum moleculare of the dentate gyrus in which the $GABA_A$/cBZ receptor density remained

increased, perhaps reflecting its gate-keeping function (Vivash et al., 2011). The general decrease at later time-points is consistent with findings from a study using ^{123}I-Iomazenil in the intrahippocampal KASE model (Tamagami et al., 2004) and in a seizure-susceptible model of cortical dysplasia (Morimoto et al., 2004).

For serial PET studies during epileptogenesis, non-invasive quantification and validated simplified quantification methods are important. Liefaard and colleagues developed a population pharmacokinetic model to quantify both the receptor density (Bmax) and affinity (Kd) of the receptor complex from a PET study using a single ^{11}C-FMZ bolus injection and femoral artery-derived arterial input function measurements (Liefaard et al., 2005). This model is based on the injection of a range of doses, from a tracer dose to saturation of the receptor, in different subjects. Using this method, they found a 36% decrease in the receptor density in fully kindled rats (Liefaard et al., 2009). A second study from their group reported a modest decrease in $GABA_A$/cBZ receptor density in the KASE model at 2 and 7 days after SE (Syvanen et al., 2012).

^{11}C-labeled radioligands resulted in a few drawbacks given their fast radioactive decay (20.3 min) and the requirement of an on-site cyclotron. The use of ^{18}F-labeled radioligands offered a higher specific activity (high ratio of labeled to unlabeled ligand) as ^{18}F has a slower decay (109.8 min) compared to ^{11}C (20.3 min). An additional translational advantage of working with fluorinated radioligands is the potential widespread clinical application because there is no requirement for an on-site cyclotron. Therefore, the use of ^{18}F-labeled FMZ began to be investigated (Dedeurwaerdere et al., 2009). Non-invasive quantification methods were developed following validation with invasive protocols to measure arterial input function (Vivash et al., 2014). Briefly, for full quantification, a multi-injection experiment was performed in healthy animals. Injection of a tracer with partial and full saturating doses together with sampling of arterial input function allowed to determine the $GABA_A$ /cBZR Bmax and Kd using a two-tissue compartmental model. Based on derivation of the kinetic parameters from the multi-injection experiment, it was possible to validate the modeling approach of the partial saturation model previously implemented for ^{11}C-FMZ PET in humans (Delforge et al., 1995). This method relies on the observation that flumazenil kinetics in the cerebral tissue achieve a dynamic ‘‘Scatchard-like equilibrium’’ after injection of a mass that ensures at least 50% to 70% occupancy of the receptors. This method is non-invasive when a

reference region is used to estimate the concentration of the radioligand in the free compartment. Application of this model to KASE rats during the chronic epilepsy phase (6 weeks after SE) revealed a decrease in the $GABA_A$/cBZ receptor density in the hippocampus *in vivo* (Vivash et al., 2014). This is consistent with previous *post-mortem* studies in epilepsy models (Vivash et al., 2011) and several clinical studies in focal epilepsy (Goethals et al., 2003). In a clinical follow-up study, decreased binding of ^{18}F-FMZ in the epileptogenic zone of patients with TLE or extra-temporal epilepsy appeared to be more confined than that observed with FDG-PET (Vivash et al., 2013).

Along with glucose hypometabolism, the contribution of cell loss to the decreases observed in FMZ PET must be considered. Particularly in hippocampal sclerosis, there is neuronal loss that may result in a reduction of $GABA_A$/cBZ receptor. An earlier study from Vivash and colleagues measured the *post-mortem* $GABA_A$/cBZ receptor density with ^{3}H-FMZ autoradiography, showing a reduction in the $GABA_A$/cBZ receptor density in CA3c in the KASE model, which normalized when corrected for neuronal loss (Vivash et al., 2011). *In vivo*, no correlations were detected between the $GABA_A$/cBZ receptor density measured with ^{18}F-FMZ PET and the hippocampal volume on MRI or neuronal loss detected histologically *post-mortem* (Vivash et al., 2014). Also in human studies, a conclusive relation between cell loss and FMZ PET has not been observed (Hand et al., 1997; Koepp et al., 1997; Bouvard et al., 2005). In the kindling model, a decrease in FMZ binding is also observed without gross cell loss, but it is not always consistent. In MRI-negative patients, FMZ PET abnormalities are also variable (increases and decreases) and not always related to the epileptogenic zone (Koepp et al., 2000; Hammers et al., 2002). A reduction in $GABA_A$/cBZ receptor density may occur due to the internalization of receptors following extensive receptor stimulation (Blair et al., 2004) or in the projection areas as a consequence of a loss of synaptic connectivity due to neuronal loss in input regions such as the hippocampus. FMZ PET will only reflect alterations in receptor density and affinity, but not in function. This is relevant when considering reports that $GABA_A$ receptors can become excitatory in epilepsy (Lamsa and Taira, 2003; Wright et al., 2011).

In addition to $GABA_A$ receptor, dopamine receptors and dopaminergic neurotransmitters are frequently studied in the context of psychiatric conditions. Also in a post-SE model, decreased availability of dopamine receptors 2 and 3 ($D_{2/3}R$) was demonstrated with ^{18}F-

fallypride PET in the chronic phase (Yakushev et al., 2010). The reduced $D_{2/3}R$ availability may be due to an increased dopaminergic tone associated with seizure activity that is known to occur in epilepsy (Starr, 1996). This is relevant as studies have indicated a role for D_2 receptors in seizure generalization (Bozzi and Borrelli, 2002). In addition, these results may be relevant for some of the behavioral deficits observed in animal models of TLE.

Although glutamatergic neurotransmission plays a major role in epilepsy, only a few nuclear imaging studies have been performed due to the limited availability of radioligands targeting the glutamatergic system with suitable properties for *in vivo* neuroimaging. Choi and colleagues studied metabotropic glutamate receptor 5 (mGluR5) changes at three time-points during epileptogenesis (1 day, 1 week and 3 weeks post-SE) in different cohorts of rats after pilocarpine-induced SE (Choi et al., 2014b). In the acute stage (1 day post-SE), they found a global decrease in ^{11}C-ABP688 binding, which recovered during the subsequent imaging time-points, but remained decreased in the amygdala and hippocampus 3 weeks post-SE (Choi et al., 2014b). The global decrease 1 day after SE indicates that mGluR5 reduction is not only due to cell loss, which is expected to occur more focally. Another study found decreased mGluR5 levels after SE, showing changes in long-term depression in parallel that may be relevant for elimination of superfluous synapses (Kirschstein et al., 2007). In contrast, in TLE patients, an increase in mGluR5 per neuron was observed with immunohistochemistry (Notenboom et al., 2006). As increases in mGluR5 are also observed on activated astrocytes with immunohistochemistry (Aronica et al., 2000), this may further complicate the interpretation of ^{11}C-ABP688 binding *in vivo*. In addition to mGluRs, also ionotropic glutamate receptors are of interest. A recent study validated *ex vivo* ^{18}F-GE-179 and ^{18}F-GE-194, radiotracers targeting open/active N-methyl-D-aspartate (NMDA) and $GABA_A$ receptors respectively, in a post-traumatic brain injury rat model where they showed subacute and chronic increases in proximity of the injury (Lopez-Picon et al., 2016). Interestingly, McGinnity and colleagues showed increase NMDA binding in the hippocampus of patients with TLE using ^{18}F-GE-179 (McGinnity et al., 2015), which may reflect increased excitability.

Imaging brain inflammation and drug resistance

Brain inflammation is a common feature of most types of epilepsies and it is characterized by the production of a cascade of inflammatory mediators. Microglia, astrocytes, neurons, BBB, endothelial cells, and peripheral immune cells extravasating into brain parenchyma can all produce pro-inflammatory and anti-inflammatory molecules (Vezzani et al., 2011a).
Previous studies showed that brain inflammation occurs during epileptogenesis (Vezzani et al., 2013) and contributes to seizure generation in animal models of epilepsy (Vezzani et al., 2011a; Vezzani et al., 2011b). These findings suggest that brain inflammation plays a role in the development of epilepsy and represents a potential mechanism of epileptogenesis and ictogenesis (Pitkanen et al., 2016).
To date, the main approach to visualize brain inflammation *in vivo* is based on targeting specific molecules expressed by immune-specific cells (Amhaoul et al., 2014). In particular, a lot of attention has been devoted to the translocator protein 18kDa (TSPO), a protein located in the outer membrane of the mitochondria involved in a wide array of functions, although its precise physiological function is still unknown (Selvaraj and Stocco, 2015). Expression of TSPO in healthy brain tissue is very low and TSPO levels increase under inflammatory conditions, offering a prominent hallmark of brain inflammation.

In the first study using the KASE model, binding of ^{18}F-PBR111, a second-generation and specific TSPO ligand, was quantified 1 week after SE by modeling the dynamic PET data with a two-compartmental model with an arterial input function (Dedeurwaerdere et al., 2012). The spatial pattern of *in vivo* TSPO binding in the brain, which was particularly increased in the limbic system, matched the TSPO binding measured by *in vitro* and *ex vivo* autoradiography. As further validation, the estimated TSPO distribution volume *in vivo* correlated with TSPO expression quantified by *post-mortem* autoradiography. As the use of an invasive arterial input function is not suitable for longitudinal studies, a simplified quantification method was derived based on the radioactivity in the brain and a single metabolite-corrected plasma sample. Recently, the use of kinetic modeling to determine binding potential of ^{11}C-PK11195 (a first generation ligand of TSPO) using a simplified reference tissue model with the cerebellar grey matter as the reference region was demonstrated to correlate well with *in vitro* autoradiography (Brackhan et al., 2016). Other studies in the KASE and pilocarpine models confirmed that TSPO expression in the brain during epileptogenesis evolves with a precise spatiotemporal profile, peaking at 1-2 weeks

post-SE (Amhaoul et al., 2015; Brackhan et al., 2016; Yankam Njiwa et al., 2016). Remarkably, a recent study showed that TSPO PET can differentiate subpopulations of animals with different seizure burden at onset of epilepsy (2 weeks post-SE). By applying a multivariate data-driven modeling approach on ^{18}F-PBR111 SUV at disease onset, it is possible to accurately predict ($R = 0.92$; $R^2 = 0.86$) SRS frequency for each KASE rat monitored by continuous video-EEG recordings over 12 weeks (Bertoglio et al., 2017) (Fig. 4). In addition, the authors demonstrated that TSPO expression at early stages of disease (2 and 4 weeks post-SE) reflects the severity of depression-like and sensorimotor-related comorbidities during chronic epilepsy (Bertoglio et al., 2017).

In the chronic epilepsy phase, increased levels of TSPO expression are still detectable with *in vivo* PET 6 weeks after SE (Amhaoul et al., 2015) as well as 10 weeks post-SE (Russmann et al., 2017). Brackhan and colleagues showed that increased TSPO levels were detectable with ^{11}C-PK11195 PET 14-16 weeks after SE in a subset of animals (2 - 4) in the pilocarpine model, but this was not significant at the group level with this small number of animals (Brackhan et al., 2016). *Post-mortem* studies show that 12 weeks after SE, expression of TSPO is more confined and particularly elevated in sub-regions of the hippocampus (CA1 and hilus) and piriform cortex in the KASE model, which could reflect the seizure onset zone (Amhaoul et al., 2015). In the same study, TSPO levels were correlated with spontaneous recurrent seizures, suggesting that TSPO could be used as a biomarker for epilepsy.

Brain inflammation is a multifactorial process and has different functions, including pro- or anti-inflammatory actions, and the effect on the pathologic condition can be beneficial or detrimental depending on the circumstances. Therefore, new radiotracers for several components of the inflammatory process are warranted. Despite being one of the most common biomarkers of brain inflammation in epilepsy and other brain disorders, the function of TSPO under inflammatory conditions is ambiguous. In addition, there is very limited information regarding how TSPO expression changes in relation to the pro- or anti-inflammatory phenotype of the microglia or in response to anti-inflammatory drugs. For instance, a recent study investigating the effects of the cytokine interleukin 13 to induce the anti-inflammatory phenotype (M2) of the microglia showed that TSPO was also expressed on M2 microglia/microphages (Ali et al., 2017). TSPO function under inflammatory conditions and its expression changes are important questions for future studies.

Preclinical data suggest that TSPO PET could be used as a tool to assess treatment efficacy (Bar-Klein et al., 2016) and study drug resistance in epilepsy (Bogdanovic et al., 2014). Bar-Klein and colleagues reported significantly lower levels of TSPO in rats when exposed to isoflurane 5 days following intrahippocampal injection of KA. In addition, treatment with isoflurane resulted in a significantly lower proportion of animals developing SRS (Bar-Klein et al., 2016). In chronic epilepsy (12 weeks after electrically sustained SE), no overall difference was observed between control and epileptic animals in TSPO binding of ^{11}C-PK11195. However, uptake of ^{11}C-PK11195 was increased in rats that did not respond to phenobarbital treatment, whereas no distinction could be made between responders and non-responders based on ^{18}F-FDG scans. As these non-responder animals also had a higher number of seizures before treatment compared to the phenobarbital-responding rats, it is not clear yet whether ^{11}C-PK11195 uptake reflects intrinsic disease severity or drug resistance.

Another PET target that has received attention is the P-glycoprotein (P-gp) in order to investigate enhanced P-gp activity, a putative mechanism of drug resistance. Small animal PET studies in post-SE models have made use of PET tracers that are P-gp substrates or inhibitors (i.e. ^{18}F-MPPF, ^{11}C-verapamil, ^{11}C-quinidine, and ^{11}C-laniquidar) (Bartmann et al., 2010; Bankstahl et al., 2011; Syvanen et al., 2011; Mullauer et al., 2012; Syvanen et al., 2013). Administration of tariquidar, (a P-gp inhibitor) before scanning enhances the discrimination of group differences in kinetic influx/efflux rate constants ($k1$ and $k2$) of ^{11}C-quinidine and ^{11}C-verapamil between control and epilepsy groups (Bankstahl et al., 2011; Mullauer et al., 2012; Syvanen et al., 2013), suggesting that P-gp activity is altered in epilepsy models. In addition, pre-treatment with tariquidar allowed for differentiation between responders and non-responders in a model of pharmacoresistent epilepsy with ^{11}C-quinidine and ^{18}F-MPPF (Bartmann et al., 2010; Syvanen et al., 2013).

CONCLUSION AND PERSPECTIVES

As highlighted in this review, *in vivo* imaging represents a non-invasive and clinically translatable technique that can contribute in the identification of early biomarkers, longitudinal monitoring of disease progression, and evaluation of effectiveness of anti-epileptogenic or disease-modifying therapies. Different imaging approaches such as

microstructural MRI, fMRI, PET, and SPECT are capable of assessing and quantifying several different changes after various brain insults leading to epilepsy. For these reasons, non-invasive imaging is an important tool for epilepsy research and it will become more and more important in preclinical trials. Appropriate non-invasive susceptibility biomarkers could be used to select animals with a high epilepsy risk, and play a role in the development and evaluation of new treatments for epilepsy.

A common limitation of current imaging studies in epilepsy models is the lack of specificity for epileptogenesis processes. Indeed, it is not always examined whether the alterations observed are the results of the epileptogenic process or they are related to the initial brain insult. In addition, several studies lack video-EEG monitoring to confirm the occurrence and frequency of spontaneous recurrent seizures, as a result they could not investigate a correlation with epileptogenesis.

Given the multifactorial nature of epilepsy, the investigation of different factors in parallel could offer a deeper insight in the process of epileptogenesis. Factors, such as cell loss, BBB dysfunction or altered perfusion should be considered. Based on these considerations, multi-modal imaging (PET/MRI) could provide valuable and complementary information of the epileptogenic processes. PET/MRI scanners could potentially identify heterogeneity and evolving phenotypes in disease progression, greatly advancing *in vivo* imaging of the brain by visualizing morphological, functional, and molecular changes.

Future studies will need to be carefully designed, adequately powered, utilize advances in image acquisition and post-processing. Moreover, combining (multi-modal) imaging data with other validated techniques (e.g. video-EEG monitoring and behavioral assessment) will allow further improvements towards a better understanding of the epileptogenic process and the development of interventions that are effective at preventing or reversing epilepsy.

Acknowledgements

DB has a PhD fellowship from the Research Foundation Flanders (FWO, 11W2516N), OG is supported by Academy of Finland.

REFERENCES

Ali I, Aertgeerts S, Le Blon D, Bertoglio D, Hoornaert C, Ponsaerts P, Dedeurwaerdere S (2017) Intracerebral delivery of the M2 polarizing cytokine interleukin 13 using mesenchymal stem cell implants in a model of temporal lobe epilepsy in mice. Epilepsia 58:1063-1072.

Alvestad S, Goa PE, Qu H, Risa O, Brekken C, Sonnewald U, Haraldseth O, Hammer J, Ottersen OP, Haberg A (2007) In vivo mapping of temporospatial changes in manganese enhancement in rat brain during epileptogenesis. Neuroimage 38:57-66.

Amhaoul H, Staelens S, Dedeurwaerdere S (2014) Imaging brain inflammation in epilepsy. Neuroscience 279:238-252.

Amhaoul H, Hamaide J, Bertoglio D, Reichel SN, Verhaeghe J, Geerts E, Van Dam D, De Deyn PP, Kumar-Singh S, Katsifis A, Van Der Linden A, Staelens S, Dedeurwaerdere S (2015) Brain inflammation in a chronic epilepsy model: Evolving pattern of the translocator protein during epileptogenesis. Neurobiol Dis 82:526-539.

Aronica E, van Vliet EA, Mayboroda OA, Troost D, da Silva FH, Gorter JA (2000) Upregulation of metabotropic glutamate receptor subtype mGluR3 and mGluR5 in reactive astrocytes in a rat model of mesial temporal lobe epilepsy. Eur J Neurosci 12:2333-2344.

Baltes C, Radzwill N, Bosshard S, Marek D, Rudin M (2009) Micro MRI of the mouse brain using a novel 400 MHz cryogenic quadrature RF probe. NMR Biomed 22:834-842.

Bankstahl JP, Bankstahl M, Kuntner C, Stanek J, Wanek T, Meier M, Ding XQ, Muller M, Langer O, Loscher W (2011) A novel positron emission tomography imaging protocol

identifies seizure-induced regional overactivity of P-glycoprotein at the blood-brain barrier. J Neurosci 31:8803-8811.

Bar-Klein G, Klee R, Brandt C, Bankstahl M, Bascunana P, Tollner K, Dalipaj H, Bankstahl JP, Friedman A, Loscher W (2016) Isoflurane prevents acquired epilepsy in rat models of temporal lobe epilepsy. Ann Neurol 80:896-908.

Bartmann H, Fuest C, la Fougere C, Xiong G, Just T, Schlichtiger J, Winter P, Boning G, Wangler B, Pekcec A, Soerensen J, Bartenstein P, Cumming P, Potschka H (2010) Imaging of P-glycoprotein-mediated pharmacoresistance in the hippocampus: proof-of-concept in a chronic rat model of temporal lobe epilepsy. Epilepsia 51:1780-1790.

Bascunana P, Javela J, Delgado M, Fernandez de la Rosa R, Shiha AA, Garcia-Garcia L, Pozo MA (2016) [(18)F]FDG PET Neuroimaging Predicts Pentylenetetrazole (PTZ) Kindling Outcome in Rats. Mol Imaging Biol 18:733-740.

Bertoglio D, Verhaeghe J, Santermans E, Amhaoul H, Jonckers E, Wyffels L, Van Der Linden A, Hens N, Staelens S, Dedeurwaerdere S (2017) Non-invasive PET imaging of brain inflammation at disease onset predicts spontaneous recurrent seizures and reflects comorbidities. Brain Behav Immun 61:69-79.

Blair RE, Sombati S, Lawrence DC, McCay BD, DeLorenzo RJ (2004) Epileptogenesis causes acute and chronic increases in GABAA receptor endocytosis that contributes to the induction and maintenance of seizures in the hippocampal culture model of acquired epilepsy. J Pharmacol Exp Ther 310:871-880.

Blumenfeld H (2007) Functional MRI studies of animal models in epilepsy. Epilepsia 48 Suppl 4:18-26.

Bogdanovic RM, Syvanen S, Michler C, Russmann V, Eriksson J, Windhorst AD, Lammertsma AA, de Lange EC, Voskuyl RA, Potschka H (2014) (R)-[11C]PK11195 brain uptake as a biomarker of inflammation and antiepileptic drug resistance: evaluation in a rat epilepsy model. Neuropharmacology 85:104-112.

Bouilleret V, Nehlig A, Marescaux C, Namer IJ (2000) Magnetic resonance imaging follow-up of progressive hippocampal changes in a mouse model of mesial temporal lobe epilepsy. Epilepsia 41:642-650.

Bouilleret V, Cardamone L, Liu C, Koe AS, Fang K, Williams JP, Myers DE, O'Brien TJ, Jones NC (2011) Confounding neurodegenerative effects of manganese for in vivo MR imaging in rat models of brain insults. J Magn Reson Imaging 34:774-784.

Bouvard S, Costes N, Bonnefoi F, Lavenne F, Mauguiere F, Delforge J, Ryvlin P (2005) Seizure-related short-term plasticity of benzodiazepine receptors in partial epilepsy: a [11C]flumazenil-PET study. Brain 128:1330-1343.

Bozzi Y, Borrelli E (2002) Dopamine D2 receptor signaling controls neuronal cell death induced by muscarinic and glutamatergic drugs. Mol Cell Neurosci 19:263-271.

Brackhan M, Bascunana P, Postema JM, Ross TL, Bengel FM, Bankstahl M, Bankstahl JP (2016) Serial quantitative TSPO-targeted PET reveals peak microglial activation up to two weeks after an epileptogenic brain insult. J Nucl Med.

Breuer H, Meier M, Schneefeld S, Hartig W, Wittneben A, Markel M, Ross TL, Bengel FM, Bankstahl M, Bankstahl JP (2017) Multimodality imaging of blood-brain barrier impairment during epileptogenesis. J Cereb Blood F Met 37:2049-2061.

Chassagnon S, Andre V, Koning E, Ferrandon A, Nehlig A (2006) Optimal window for ictal blood flow mapping. Insight from the study of discrete temporo-limbic seizures in rats. Epilepsy Res 69:100-118.

Choi H, Kim YK, Kang H, Lee H, Im HJ, Hwang do W, Kim EE, Chung JK, Lee DS (2014a) Abnormal metabolic connectivity in the pilocarpine-induced epilepsy rat model: a multiscale network analysis based on persistent homology. Neuroimage 99:226-236.

Choi H, Kim YK, Oh SW, Im HJ, Hwang do W, Kang H, Lee B, Lee YS, Jeong JM, Kim EE, Chung JK, Lee DS (2014b) In vivo imaging of mGluR5 changes during epileptogenesis using [11C]ABP688 PET in pilocarpine-induced epilepsy rat model. PLoS One 9:e92765.

Choy M, Wells JA, Thomas DL, Gadian DG, Scott RC, Lythgoe MF (2010) Cerebral blood flow changes during pilocarpine-induced status epilepticus activity in the rat hippocampus. Exp Neurol 225:196-201.

Choy M, Dube CM, Patterson K, Barnes SR, Maras P, Blood AB, Hasso AN, Obenaus A, Baram TZ (2014) A novel, noninvasive, predictive epilepsy biomarker with clinical potential. J Neurosci 34:8672-8684.

Cleeren E, Casteels C, Goffin K, Janssen P, Van Paesschen W (2015) Ictal perfusion changes associated with seizure progression in the amygdala kindling model in the rhesus monkey. Epilepsia 56:1366-1375.

Cleeren E, Premereur E, Casteels C, Goffin K, Janssen P, Van Paesschen W (2016) The effective connectivity of the seizure onset zone and ictal perfusion changes in amygdala kindled rhesus monkeys. Neuroimage Clin 12:252-261.

Dedeurwaerdere S, Jupp B, O'Brien TJ (2007) Positron Emission Tomography in basic epilepsy research: a view of the epileptic brain. Epilepsia 48 Suppl 4:56-64.

Dedeurwaerdere S, Vonck K, Van Hese P, Wadman W, Boon P (2005) The acute and chronic effect of vagus nerve stimulation in genetic absence epilepsy rats from Strasbourg (GAERS). Epilepsia 46 Suppl 5:94-97.

Dedeurwaerdere S, Fang K, Chow M, Shen YT, Noordman I, van Raay L, Faggian N, Porritt M, Egan GF, O'Brien TJ (2013) Manganese-enhanced MRI reflects seizure outcome in a model for mesial temporal lobe epilepsy. Neuroimage 68:30-38.

Dedeurwaerdere S, Callaghan PD, Pham T, Rahardjo GL, Amhaoul H, Berghofer P, Quinlivan M, Mattner F, Loc'h C, Katsifis A, Gregoire MC (2012) PET imaging of brain inflammation during early epileptogenesis in a rat model of temporal lobe epilepsy. Eur J Nucl Med Mol I Res 2:60.

Dedeurwaerdere S, Gregoire MC, Vivash L, Roselt P, Binns D, Fookes C, Greguric I, Pham T, Loc'h C, Katsifis A, Hicks RJ, O'Brien TJ, Myers DE (2009) In-vivo imaging characteristics of two fluorinated flumazenil radiotracers in the rat. Eur J Nucl Med Mol I 36:958-965.

Delforge J, Pappata S, Millet P, Samson Y, Bendriem B, Jobert A, Crouzel C, Syrota A (1995) Quantification of benzodiazepine receptors in human brain using PET, [11C]flumazenil, and a single-experiment protocol. J Cereb Blood F Met 15:284-300.

Deo A, Fogel M, Cowper SE (2007) Nephrogenic systemic fibrosis: A population study examining the relationship of disease development to gadolinium exposure. Clin J Am Soc Nephro 2:264-267.

Dietrich Y, Eliat PA, Dieuset G, Saint-Jalmes H, Pineau C, Wendling F, Martin B (2016) Structural and functional changes during epileptogenesis in the mouse model of medial temporal lobe epilepsy. IEEE Eng Med Biol Soc Ann 2016:4005-4008.

Dlugos DJ, Jaggi J, O'Connor WM, Ding XS, Reivich M, O'Connor MJ, Sperling MR (1999) Hippocampal cell density and subcortical metabolism in temporal lobe epilepsy. Epilepsia 40:408-413.

Dube C, Boyet S, Marescaux C, Nehlig A (2001) Relationship between neuronal loss and interictal glucose metabolism during the chronic phase of the lithium-pilocarpine model of epilepsy in the immature and adult rat. Exp Neurol 167:227-241.

Ebisu T, Rooney WD, Graham SH, Mancuso A, Weiner MW, Maudsley AA (1996) MR spectroscopic imaging and diffusion-weighted MRI for early detection of kainate-induced status epilepticus in the rat. Magn Reson Med 36:821-828.

Engel J, Jr., Brown WJ, Kuhl DE, Phelps ME, Mazziotta JC, Crandall PH (1982) Pathological findings underlying focal temporal lobe hypometabolism in partial epilepsy. Ann Neurol 12:518-528.

Englot DJ, Modi B, Mishra AM, DeSalvo M, Hyder F, Blumenfeld H (2009) Cortical deactivation induced by subcortical network dysfunction in limbic seizures. J Neurosci 29:13006-13018.

Eschenko O, Canals S, Simanova I, Beyerlein M, Murayama Y, Logothetis NK (2010) Mapping of functional brain activity in freely behaving rats during voluntary running using manganese-enhanced MRI: implication for longitudinal studies. Neuroimage 49:2544-2555.

Fabene PF, Marzola P, Sbarbati A, Bentivoglio M (2003) Magnetic resonance imaging of changes elicited by status epilepticus in the rat brain: diffusion-weighted and T2-weighted images, regional blood volume maps, and direct correlation with tissue and cell damage. Neuroimage 18:375-389.

Fabene PF, Weiczner R, Marzola P, Nicolato E, Calderan L, Andrioli A, Farkas E, Sule Z, Mihaly A, Sbarbati A (2006) Structural and functional MRI following 4-aminopyridine-induced seizures: a comparative imaging and anatomical study. Neurobiol Dis 21:80-89.

Filibian M, Frasca A, Maggioni D, Micotti E, Vezzani A, Ravizza T (2012) In vivo imaging of glia activation using 1H-magnetic resonance spectroscopy to detect putative biomarkers of tissue epileptogenicity. Epilepsia 53:1907-1916.

Gao F, Guo Y, Zhang H, Wang S, Wang J, Wu JM, Chen Z, Ding MP (2009) Anterior thalamic nucleus stimulation modulates regional cerebral metabolism: an FDG-MicroPET study in rats. Neurobiol Dis 34:477-483.

Garcia-Garcia L, Shiha AA, Bascunana P, de Cristobal J, Fernandez de la Rosa R, Delgado M, Pozo MA (2016) Serotonin Depletion Does not Modify the Short-Term Brain Hypometabolism and Hippocampal Neurodegeneration Induced by the Lithium-Pilocarpine Model of Status Epilepticus in Rats. Cell Mol Neurobiol 36:513-519.

Garcia-Garcia L, Shiha AA, Fernandez de la Rosa R, Delgado M, Silvan A, Bascunana P, Bankstahl JP, Gomez F, Pozo MA (2017) Metyrapone prevents brain damage induced by status epilepticus in the rat lithium-pilocarpine model. Neuropharmacology.

Gill RS, Mirsattari SM, Leung LS (2017) Resting state functional network disruptions in a kainic acid model of temporal lobe epilepsy. Neuroimage Clin 13:70-81.

Goethals I, Van de Wiele C, Boon P, Dierckx R (2003) Is central benzodiazepine receptor imaging useful for the identification of epileptogenic foci in localization-related epilepsies? Eur J Nucl Med Mol I 30:325-328.

Goffin K, Dedeurwaerdere S, Van Laere K, Van Paesschen W (2008) Neuronuclear assessment of patients with epilepsy. Semin Nucl Med 38:227-239.

Goffin K, Van Paesschen W, Dupont P, Van Laere K (2009) Longitudinal microPET imaging of brain glucose metabolism in rat lithium-pilocarpine model of epilepsy. Exp Neurol 217:205-209.

Gomes WA, Lado FA, de Lanerolle NC, Takahashi K, Pan C, Hetherington HP (2007) Spectroscopic imaging of the pilocarpine model of human epilepsy suggests that early NAA reduction predicts epilepsy. Magn Reson Med 58:230-235.

Gozzi A, Schwarz AJ (2016) Large-scale functional connectivity networks in the rodent brain. Neuroimage 127:496-509.

Grohn O, Sierra A, Immonen R, Laitinen T, Lehtimaki K, Airaksinen A, Hayward N, Nairismagi J, Lehto L, Pitkanen A (2011) Multimodal MRI assessment of damage and plasticity caused by status epilepticus in the rat brain. Epilepsia 52 Suppl 8:57-60.

Guo Y, Gao F, Wang S, Ding Y, Zhang H, Wang J, Ding MP (2009) In vivo mapping of temporospatial changes in glucose utilization in rat brain during epileptogenesis: an 18F-fluorodeoxyglucose-small animal positron emission tomography study. Neuroscience 162:972-979.

Hamamoto Y, Hasegawa D, Mizoguchi S, Yu Y, Wada M, Kuwabara T, Fujiwara-Igarashi A, Fujita M (2017) Changes in the interictal and early postictal diffusion and perfusion magnetic resonance parameters in familial spontaneous epileptic cats. Epilepsy Res 133:76-82.

Hammers A, Koepp MJ, Hurlemann R, Thom M, Richardson MP, Brooks DJ, Duncan JS (2002) Abnormalities of grey and white matter [11C]flumazenil binding in temporal lobe epilepsy with normal MRI. Brain 125:2257-2271.

Hand KS, Baird VH, Van Paesschen W, Koepp MJ, Revesz T, Thom M, Harkness WF, Duncan JS, Bowery NG (1997) Central benzodiazepine receptor autoradiography in hippocampal sclerosis. Brit J Pharmacol 122:358-364.

Hayward NM, Ndode-Ekane XE, Kutchiashvili N, Grohn O, Pitkanen A (2010) Elevated cerebral blood flow and vascular density in the amygdala after status epilepticus in rats. Neurosci Lett 484:39-42.

Hayward NM, Tuunanen PI, Immonen R, Ndode-Ekane XE, Pitkanen A, Grohn O (2011) Magnetic resonance imaging of regional hemodynamic and cerebrovascular recovery after lateral fluid-percussion brain injury in rats. J Cereb Blood F Met 31:166-177.

Henry TR (1996) Functional neuroimaging with positron emission tomography. Epilepsia 37:1141-1154.

Hsu YH, Lee WT, Chang C (2007) Multiparametric MRI evaluation of kainic acid-induced neuronal activation in rat hippocampus. Brain 130:3124-3134.

Hume SP, Jones T (1998) Positron emission tomography (PET) methodology for small animals and its application in radiopharmaceutical preclinical investigation. Nucl Med Biol 25:729-732.

Immonen R, Kharatishvili I, Grohn O, Pitkanen A (2013) MRI biomarkers for post-traumatic epileptogenesis. J Neurotraum 30:1305-1309.

Immonen RJ, Kharatishvili I, Grohn H, Pitkanen A, Grohn OH (2009b) Quantitative MRI predicts long-term structural and functional outcome after experimental traumatic brain injury. Neuroimage 45:1-9.

Immonen RJ, Kharatishvili I, Sierra A, Einula C, Pitkanen A, Grohn OH (2008) Manganese enhanced MRI detects mossy fiber sprouting rather than neurodegeneration, gliosis or seizure-activity in the epileptic rat hippocampus. Neuroimage 40:1718-1730.

Immonen RJ, Kharatishvili I, Niskanen JP, Grohn H, Pitkanen A, Grohn OH (2009a) Distinct MRI pattern in lesional and perilesional area after traumatic brain injury in rat--11 months follow-up. Exp Neurol 215:29-40.

Jonckers E, Shah D, Hamaide J, Verhoye M, Van der Linden A (2015) The power of using functional fMRI on small rodents to study brain pharmacology and disease. Front Pharmacol 6:231.

Jones-Davis DM, Macdonald RL (2003) GABA(A) receptor function and pharmacology in epilepsy and status epilepticus. Curr Opin Pharmacol 3:12-18.

Jupp B, Williams J, Binns D, Hicks RJ, Cardamone L, Jones N, Rees S, O'Brien TJ (2012) Hypometabolism precedes limbic atrophy and spontaneous recurrent seizures in a rat model of TLE. Epilepsia 53:1233-1244.

Katsifis A, Kassiou M (2004) Development of radioligands for in vivo imaging of GABA(A)-benzodiazepine receptors. Mini-Rev Med Chem 4:909-921.

Keezer MR, Sisodiya SM, Sander JW (2016) Comorbidities of epilepsy: current concepts and future perspectives. Lancet Neurol 15:106-115.

Kharatishvili I, Immonen R, Grohn O, Pitkanen A (2007) Quantitative diffusion MRI of hippocampus as a surrogate marker for post-traumatic epileptogenesis. Brain 130:3155-3168.

Kharatishvili I, Shan ZY, She DT, Foong S, Kurniawan ND, Reutens DC (2014) MRI changes and complement activation correlate with epileptogenicity in a mouse model of temporal lobe epilepsy. Brain Struct Funct 219:683-706.

Kim YB, Kalthoff D, Po C, Wiedermann D, Hoehn M (2012) Connectivity of thalamo-cortical pathway in rat brain: combined diffusion spectrum imaging and functional MRI at 11.7 T. NMR Biomed 25:943-952.

Kirschstein T, Bauer M, Muller L, Ruschenschmidt C, Reitze M, Becker AJ, Schoch S, Beck H (2007) Loss of metabotropic glutamate receptor-dependent long-term depression via downregulation of mGluR5 after status epilepticus. J Neurosci 27:7696-7704.

Koepp MJ, Hammers A, Labbe C, Woermann FG, Brooks DJ, Duncan JS (2000) 11C-flumazenil PET in patients with refractory temporal lobe epilepsy and normal MRI. Neurology 54:332-339.

Koepp MJ, Richardson MP, Labbe C, Brooks DJ, Cunningham VJ, Ashburner J, Van Paesschen W, Revesz T, Duncan JS (1997) 11C-flumazenil PET, volumetric MRI, and quantitative pathology in mesial temporal lobe epilepsy. Neurology 49:764-773.

Kornblum HI, Araujo DM, Annala AJ, Tatsukawa KJ, Phelps ME, Cherry SR (2000) In vivo imaging of neuronal activation and plasticity in the rat brain by high resolution positron emission tomography (microPET). Nat Biotechnol 18:655-660.

Kuo LW, Lee CY, Chen JH, Wedeen VJ, Chen CC, Liou HH, Tseng WY (2008) Mossy fiber sprouting in pilocarpine-induced status epilepticus rat hippocampus: a correlative study of diffusion spectrum imaging and histology. Neuroimage 41:789-800.

Laitinen T, Sierra A, Pitkanen A, Grohn O (2010) Diffusion tensor MRI of axonal plasticity in the rat hippocampus. Neuroimage 51:521-530.

Lamsa K, Taira T (2003) Use-dependent shift from inhibitory to excitatory GABAA receptor action in SP-O interneurons in the rat hippocampal CA3 area. J Neurophysiol 90:1983-1995.

Lee EM, Park GY, Im KC, Kim ST, Woo CW, Chung JH, Kim KS, Kim JS, Shon YM, Kim YI, Kang JK (2012) Changes in glucose metabolism and metabolites during the epileptogenic process in the lithium-pilocarpine model of epilepsy. Epilepsia 53:860-869.

Liefaard LC, Ploeger BA, Molthoff CF, Boellaard R, Lammertsma AA, Danhof M, Voskuyl RA (2005) Population pharmacokinetic analysis for simultaneous determination of B

(max) and K (D) in vivo by positron emission tomography. Mol Imaging Biol 7:411-421.

Liefaard LC, Ploeger BA, Molthoff CF, de Jong HW, Dijkstra J, van der Weerd L, Lammertsma AA, Danhof M, Voskuyl RA (2009) Changes in GABAA receptor properties in amygdala kindled animals: in vivo studies using [11C]flumazenil and positron emission tomography. Epilepsia 50:88-98.

Liu DS, O'Brien TJ, Williams DA, Hicks RJ, Myers DE (2009) Lamina-specific changes in hippocampal GABA(A)/cBZR and mossy fibre sprouting during and following amygdala kindling in the rat. Neurobiol Dis 35:337-347.

Liu SJ, Zheng P, Wright DK, Dezsi G, Braine E, Nguyen T, Corcoran NM, Johnston LA, Hovens CM, Mayo JN, Hudson M, Shultz SR, Jones NC, O'Brien TJ (2016) Sodium selenate retards epileptogenesis in acquired epilepsy models reversing changes in protein phosphatase 2A and hyperphosphorylated tau. Brain 139:1919-1938.

Long Q, Li J, Luo Q, Hei Y, Wang K, Tian Y, Yang J, Lei H, Qiu B, Liu W (2015) MRI tracking of bone marrow mesenchymal stem cells labeled with ultra-small superparamagnetic iron oxide nanoparticles in a rat model of temporal lobe epilepsy. Neurosci Lett 606:30-35.

Lopez-Picon F, Snellman A, Shatillo O, Lehtiniemi P, Gronroos TJ, Marjamaki P, Trigg W, Jones PA, Solin O, Pitkanen A, Haaparanta-Solin M (2016) Ex Vivo Tracing of NMDA and GABA-A Receptors in Rat Brain After Traumatic Brain Injury Using 18F-GE-179 and 18F-GE-194 Autoradiography. J Nucl Med 57:1442-1447.

Malheiros JM, Paiva FF, Longo BM, Hamani C, Covolan L (2015) Manganese-enhanced MRI: biological applications in neuroscience. Front Neurol 6:161.

Malheiros JM, Persike DS, Castro LU, Sanches TR, Andrade Lda C, Tannus A, Covolan L (2014) Reduced hippocampal manganese-enhanced MRI (MEMRI) signal during pilocarpine-induced status epilepticus: edema or apoptosis? Epilepsy Res 108:644-652.

McGinnity CJ, Koepp MJ, Hammers A, Riano Barros DA, Pressler RM, Luthra S, Jones PA, Trigg W, Micallef C, Symms MR, Brooks DJ, Duncan JS (2015) NMDA receptor binding in focal epilepsies. J Neurol Neurosur Ps 86:1150-1157.

Mena I, Marin O, Fuenzalida S, Cotzias GC (1967) Chronic Manganese Poisoning - Clinical Picture and Manganese Turnover. Neurology 17:128-+.

Mirrione MM, Tsirka SE (2011) Neuroimaging in Animal Seizure Models with (18)FDG-PET. Epilepsy Res Treat 2011:369295.

Mirrione MM, Schiffer WK, Siddiq M, Dewey SL, Tsirka SE (2006) PET imaging of glucose metabolism in a mouse model of temporal lobe epilepsy. Synapse 59:119-121.

Mirrione MM, Schiffer WK, Fowler JS, Alexoff DL, Dewey SL, Tsirka SE (2007) A novel approach for imaging brain-behavior relationships in mice reveals unexpected metabolic patterns during seizures in the absence of tissue plasminogen activator. Neuroimage 38:34-42.

Mishra AM, Bai X, Sanganahalli BG, Waxman SG, Shatillo O, Grohn O, Hyder F, Pitkanen A, Blumenfeld H (2014) Decreased resting functional connectivity after traumatic brain injury in the rat. PLoS One 9:e95280.

Mizoguchi S, Hasegawa D, Hamamoto Y, Yu Y, Kuwabara T, Fujiwara-Igarashi A, Fujita M (2017) Interictal diffusion and perfusion magnetic resonance imaging features of cats with familial spontaneous epilepsy. Am J Vet Res 78:305-310.

Montgomery AJ, Thielemans K, Mehta MA, Turkheimer F, Mustafovic S, Grasby PM (2006) Correction of head movement on PET studies: comparison of methods. J Nucl Med 47:1936-1944.

Mori S, Zhang JY (2006) Principles of diffusion tensor imaging and its applications to basic neuroscience research. Neuron 51:527-539.

Morimoto K, Watanabe T, Ninomiya T, Hirao T, Tanaka A, Onishi T, Tamagami H (2004) Quantitative evaluation of central-type benzodiazepine receptors with [(125)I]Iomazenil in experimental epileptogenesis: II. The rat cortical dysplasia model. Epilepsy Res 61:113-118.

Moseley ME, Kucharczyk J, Mintorovitch J, Cohen Y, Kurhanewicz J, Derugin N, Asgari H, Norman D (1990) Diffusion-weighted MR imaging of acute stroke: correlation with T2-weighted and magnetic susceptibility-enhanced MR imaging in cats. Am J Neuroradiol 11:423-429.

Motelow JE, Li W, Zhan Q, Mishra AM, Sachdev RN, Liu G, Gummadavelli A, Zayyad Z, Lee HS, Chu V, Andrews JP, Englot DJ, Herman P, Sanganahalli BG, Hyder F, Blumenfeld H (2015) Decreased subcortical cholinergic arousal in focal seizures. Neuron 85:561-572.

Mullauer J, Kuntner C, Bauer M, Bankstahl JP, Muller M, Voskuyl RA, Langer O, Syvanen S (2012) Pharmacokinetic modeling of P-glycoprotein function at the rat and human blood-brain barriers studied with (R)-[11C]verapamil positron emission tomography. ur J Nucl Med Mol I Res 2:58.

Nairismagi J, Grohn OH, Kettunen MI, Nissinen J, Kauppinen RA, Pitkanen A (2004) Progression of brain damage after status epilepticus and its association with epileptogenesis: a quantitative MRI study in a rat model of temporal lobe epilepsy. Epilepsia 45:1024-1034.

Nairismagi J, Pitkanen A, Narkilahti S, Huttunen J, Kauppinen RA, Grohn OH (2006) Manganese-enhanced magnetic resonance imaging of mossy fiber plasticity in vivo. Neuroimage 30:130-135.

Nehlig A, Obenaus A (2006) Models of Seizures and Epilepsy: Elsevier.

Niessen HG, Angenstein F, Vielhaber S, Frisch C, Kudin A, Elger CE, Heinze HJ, Scheich H, Kunz WS (2005) Volumetric magnetic resonance imaging of functionally relevant structural alterations in chronic epilepsy after pilocarpine-induced status epilepticus in rats. Epilepsia 46:1021-1026.

Notenboom RG, Hampson DR, Jansen GH, van Rijen PC, van Veelen CW, van Nieuwenhuizen O, de Graan PN (2006) Up-regulation of hippocampal metabotropic glutamate receptor 5 in temporal lobe epilepsy patients. Brain 129:96-107.

O'Brien TJ, Jupp B (2009) In-vivo imaging with small animal FDG-PET: a tool to unlock the secrets of epileptogenesis? Exp Neurol 220:1-4.

O'Neal SL, Zheng W (2015) Manganese Toxicity Upon Overexposure: a Decade in Review. Curr Environ Health Rep 2:315-328.

Otte WM, van Eijsden P, Sander JW, Duncan JS, Dijkhuizen RM, Braun KP (2012) A meta-analysis of white matter changes in temporal lobe epilepsy as studied with diffusion tensor imaging. Epilepsia 53:659-667.

Parekh MB, Carney PR, Sepulveda H, Norman W, King M, Mareci TH (2010) Early MR diffusion and relaxation changes in the parahippocampal gyrus precede the onset of spontaneous seizures in an animal model of chronic limbic epilepsy. Exp Neurol 224:258-270.

Pascente R, Frigerio F, Rizzi M, Porcu L, Boido M, Davids J, Zaben M, Tolomeo D, Filibian M, Gray WP, Vezzani A, Ravizza T (2016) Cognitive deficits and brain myo-Inositol are early biomarkers of epileptogenesis in a rat model of epilepsy. Neurobiol Dis 93:146-155.

Pearce PS, Wu Y, Rapuano A, Kelly KM, de Lanerolle N, Pan JW (2016) Metabolic injury in a variable rat model of post-status epilepticus. Epilepsia 57:1978-1986.

Penfield JG, Reilly RF (2007) What nephrologists need to know about gadolinium. Nat Clin Pract Nephr 3:654-668.

Phelps ME (2000) PET: the merging of biology and imaging into molecular imaging. J Nucl Med 41:661-681.

Pirttimaki T, Salo RA, Shatillo A, Kettunen MI, Paasonen J, Sierra A, Jokivarsi K, Leinonen V, Andrade P, Quittek S, Pitkanen A, Grohn O (2016) Implantable RF-coil with multiple electrodes for long-term EEG-fMRI monitoring in rodents. J Neurosci Meth 274:154-163.

Pitkanen A, Loscher W, Vezzani A, Becker AJ, Simonato M, Lukasiuk K, Grohn O, Bankstahl JP, Friedman A, Aronica E, Gorter JA, Ravizza T, Sisodiya SM, Kokaia M, Beck H (2016) Advances in the development of biomarkers for epilepsy. Lancet Neurol 15:843-856.

Polli RS, Malheiros JM, Dos Santos R, Hamani C, Longo BM, Tannus A, Mello LE, Covolan L (2014) Changes in Hippocampal Volume are Correlated with Cell Loss but Not with Seizure Frequency in Two Chronic Models of Temporal Lobe Epilepsy. Front Neurol 5:111.

Portnoy E, Polyak B, Inbar D, Kenan G, Rai A, Wehrli SL, Roberts TP, Bishara A, Mann A, Shmuel M, Rozovsky K, Itzhak G, Ben-Hur T, Magdassi S, Ekstein D, Eyal S (2016) Tracking inflammation in the epileptic rat brain by bi-functional fluorescent and magnetic nanoparticles. Nanomedicine-uk 12:1335-1345.

Rigotti DJ, Inglese M, Gonen O (2007) Whole-brain N-acetylaspartate as a surrogate marker of neuronal damage in diffuse neurologic disorders. Am J Neuroradiol 28:1843-1849.

Roch C, Leroy C, Nehlig A, Namer IJ (2002a) Predictive value of cortical injury for the development of temporal lobe epilepsy in 21-day-old rats: an MRI approach using the lithium-pilocarpine model. Epilepsia 43:1129-1136.

Roch C, Leroy C, Nehlig A, Namer IJ (2002b) Magnetic resonance imaging in the study of the lithium-pilocarpine model of temporal lobe epilepsy in adult rats. Epilepsia 43:325-335.

Rocha L, Ondarza-Rovira R (1999) Characterization of benzodiazepine receptor binding following kainic acid administration: an autoradiography study in rats. Neurosci Lett 262:211-214.

Russmann V, Brendel M, Mille E, Helm-Vicidomini A, Beck R, Gunther L, Lindner S, Rominger A, Keck M, Salvamoser JD, Albert NL, Bartenstein P, Potschka H (2017) Identification of brain regions predicting epileptogenesis by serial [18F]GE-180 positron emission tomography imaging of neuroinflammation in a rat model of temporal lobe epilepsy. Neuroimage Clin 15:35-44.

Sakurai M, Kurokawa H, Shimada A, Nakamura K, Miyata H, Morita T (2015) Excitatory amino acid transporter 2 downregulation correlates with thalamic neuronal death following kainic acid-induced status epilepticus in rat. Neuropathology 35:1-9.

Salmon E, Bernard Ir C, Hustinx R (2015) Pitfalls and Limitations of PET/CT in Brain Imaging. Semin Nucl Med 45:541-551.

Salo RA, Miettinen T, Laitinen T, Grohn O, Sierra A (2017) Diffusion tensor MRI shows progressive changes in the hippocampus and dentate gyrus after status epilepticus in rat - histological validation with Fourier-based analysis. Neuroimage 152:221-236.

Sayin U, Hutchinson E, Meyerand ME, Sutula T (2015) Age-dependent long-term structural and functional effects of early-life seizures: evidence for a hippocampal critical period influencing plasticity in adulthood. Neuroscience 288:120-134.

Selvaraj V, Stocco DM (2015) The changing landscape in translocator protein (TSPO) function. Trends Endocrin Met 26:341-348.

Sharma P, Wright DK, Johnston LA, Powell KL, Wlodek ME, Shultz SR, O'Brien TJ, Gilby KL (2017) Differences in white matter structure between seizure prone (FAST) and seizure resistant (SLOW) rat strains. Neurobiol Dis 104:33-40.

Shiha AA, de Cristobal J, Delgado M, Fernandez de la Rosa R, Bascunana P, Pozo MA, Garcia-Garcia L (2015) Subacute administration of fluoxetine prevents short-term brain hypometabolism and reduces brain damage markers induced by the lithium-pilocarpine model of epilepsy in rats. Brain Res Bull 111:36-47.

Shultz SR, O'Brien TJ, Stefanidou M, Kuzniecky RI (2014) Neuroimaging the epileptogenic process. Neurotherapeutics 11:347-357.

Shultz SR, Cardamone L, Liu YR, Hogan RE, Maccotta L, Wright DK, Zheng P, Koe A, Gregoire MC, Williams JP, Hicks RJ, Jones NC, Myers DE, O'Brien TJ, Bouilleret V (2013) Can structural or functional changes following traumatic brain injury in the rat predict epileptic outcome? Epilepsia 54:1240-1250.

Sierra A, Laitinen T, Grohn O, Pitkanen A (2015) Diffusion tensor imaging of hippocampal network plasticity. Brain Struct Funct 220:781-801.

Silva AC, Lee JH, Aoki I, Koretsky AP (2004) Manganese-enhanced magnetic resonance imaging (MEMRI): methodological and practical considerations. NMR Biomed 17:532-543.

Silva AC, Lee JH, Wu CW, Tucciarone J, Pelled G, Aoki I, Koretsky AP (2008) Detection of cortical laminar architecture using manganese-enhanced MRI. J Neurosci Meth 167:246-257.

Simister RJ, Woermann FG, McLean MA, Bartlett PA, Barker GJ, Duncan JS (2002) A short-echo-time proton magnetic resonance spectroscopic imaging study of temporal lobe epilepsy. Epilepsia 43:1021-1031.

Song SK, Sun SW, Ramsbottom MJ, Chang C, Russell J, Cross AH (2002) Dysmyelination revealed through MRI as increased radial (but unchanged axial) diffusion of water. Neuroimage 17:1429-1436.

Starr MS (1996) The role of dopamine in epilepsy. Synapse 22:159-194.

Suleymanova EM, Gulyaev MV, Abbasova KR (2016) Structural alterations in the rat brain and behavioral impairment after status epilepticus: An MRI study. Neuroscience 315:79-90.

Syvanen S, Luurtsema G, Molthoff CF, Windhorst AD, Huisman MC, Lammertsma AA, Voskuyl RA, de Lange EC (2011) (R)-[11C]verapamil PET studies to assess changes in P-glycoprotein expression and functionality in rat blood-brain barrier after exposure to kainate-induced status epilepticus. BMC Med Imaging 11:1.

Syvanen S, Labots M, Tagawa Y, Eriksson J, Windhorst AD, Lammertsma AA, de Lange EC, Voskuyl RA (2012) Altered GABAA receptor density and unaltered blood-brain barrier transport in a kainate model of epilepsy: an in vivo study using 11C-flumazenil and PET. J Nucl Med 53:1974-1983.

Syvanen S, Russmann V, Verbeek J, Eriksson J, Labots M, Zellinger C, Seeger N, Schuit R, Rongen M, van Kooij R, Windhorst AD, Lammertsma AA, de Lange EC, Voskuyl RA, Koepp M, Potschka H (2013) [(11)C]quinidine and [(11)C]laniquidar PET imaging in a chronic rodent epilepsy model: Impact of epilepsy and drug-responsiveness. Nucl Med Biol 40:764-775.

Tamagami H, Morimoto K, Watanabe T, Ninomiya T, Hirao T, Tanaka A, Kakumoto M (2004) Quantitative evaluation of central-type benzodiazepine receptors with [(125)I] Iomazenil in experimental epileptogenesis. I. The rat kainate model of temporal lobe epilepsy. Epilepsy Res 61:105-112.

Tokumitsu T, Mancuso A, Weinstein PR, Weiner MW, Naruse S, Maudsley AA (1997) Metabolic and pathological effects of temporal lobe epilepsy in rat brain detected by proton spectroscopy and imaging. Brain Res 744:57-67.

van der Hel WS, van Eijsden P, Bos IW, de Graaf RA, Behar KL, van Nieuwenhuizen O, de Graan PN, Braun KP (2013) In vivo MRS and histochemistry of status epilepticus-induced hippocampal pathology in a juvenile model of temporal lobe epilepsy. NMR Biomed 26:132-140.

van Eijsden P, Notenboom RG, Wu O, de Graan PN, van Nieuwenhuizen O, Nicolay K, Braun KP (2004) In vivo 1H magnetic resonance spectroscopy, T2-weighted and diffusion-weighted MRI during lithium-pilocarpine-induced status epilepticus in the rat. Brain Res 1030:11-18.

van Vliet EA, Otte WM, Gorter JA, Dijkhuizen RM, Wadman WJ (2014) Longitudinal assessment of blood-brain barrier leakage during epileptogenesis in rats. A quantitative MRI study. Neurobiol Dis 63:74-84.

van Vliet EA, Otte WM, Wadman WJ, Aronica E, Kooij G, de Vries HE, Dijkhuizen RM, Gorter JA (2016) Blood-brain barrier leakage after status epilepticus in rapamycin-treated rats I: Magnetic resonance imaging. Epilepsia 57:59-69.

Vezzani A, Pascente R, Ravizza T (2017) Biomarkers of Epileptogenesis: The Focus on Glia and Cognitive Dysfunctions. Neurochem Res.

Vezzani A, French J, Bartfai T, Baram TZ (2011a) The role of inflammation in epilepsy. Nat Rev Neurol 7:31-40.

Vezzani A, Aronica E, Mazarati A, Pittman QJ (2013) Epilepsy and brain inflammation. Exp Neurol 244:11-21.

Vezzani A, Maroso M, Balosso S, Sanchez MA, Bartfai T (2011b) IL-1 receptor/Toll-like receptor signaling in infection, inflammation, stress and neurodegeneration couples hyperexcitability and seizures. Brain Behav Immun 25:1281-1289.

Vivash L, Tostevin A, Liu DS, Dalic L, Dedeurwaerdere S, Hicks RJ, Williams DA, Myers DE, O'Brien TJ (2011) Changes in hippocampal GABAA/cBZR density during limbic epileptogenesis: relationship to cell loss and mossy fibre sprouting. Neurobiol Dis 41:227-236.

Vivash L, Gregoire MC, Lau EW, Ware RE, Binns D, Roselt P, Bouilleret V, Myers DE, Cook MJ, Hicks RJ, O'Brien TJ (2013) 18F-flumazenil: a gamma-aminobutyric acid A-specific PET radiotracer for the localization of drug-resistant temporal lobe epilepsy. J Nucl Med 54:1270-1277.

Vivash L, Gregoire MC, Bouilleret V, Berard A, Wimberley C, Binns D, Roselt P, Katsifis A, Myers DE, Hicks RJ, O'Brien TJ, Dedeurwaerdere S (2014) In vivo measurement of hippocampal GABAA/cBZR density with [18F]-flumazenil PET for the study of disease progression in an animal model of temporal lobe epilepsy. PLoS One 9:e86722.

Walls AB, Eyjolfsson EM, Schousboe A, Sonnewald U, Waagepetersen HS (2014) A subconvulsive dose of kainate selectively compromises astrocytic metabolism in the mouse brain in vivo. J Cereb Blood F Met 34:1340-1346.

Wang Y, Xu Z, Cheng H, Guo Y, Xu C, Wang S, Zhang J, Ding M, Chen Z (2014) Low-frequency stimulation inhibits epileptogenesis by modulating the early network of the limbic system as evaluated in amygdala kindling model. Brain Struct Funct 219:1685-1696.

WHO (2016) Epilepsy fact sheet. In.

Wolf OT, Dyakin V, Patel A, Vadasz C, de Leon MJ, McEwen BS, Bulloch K (2002) Volumetric structural magnetic resonance imaging (MRI) of the rat hippocampus following kainic acid (KA) treatment. Brain Res 934:87-96.

Wright R, Raimondo JV, Akerman CJ (2011) Spatial and temporal dynamics in the ionic driving force for GABA(A) receptors. Neural Plast 2011:728395.

Wu Y, Pearce PS, Rapuano A, Hitchens TK, de Lanerolle NC, Pan JW (2015) Metabolic changes in early poststatus epilepticus measured by MR spectroscopy in rats. J Cereb Blood F Met 35:1862-1870.

Wyckhuys T, De Geeter N, Crevecoeur G, Stroobants S, Staelens S (2013) Quantifying the effect of repetitive transcranial magnetic stimulation in the rat brain by muSPECT CBF scans. Brain Stimul 6:554-562.

Wyckhuys T, Staelens S, Van Nieuwenhuyse B, Deleye S, Hallez H, Vonck K, Raedt R, Wadman W, Boon P (2010) Hippocampal deep brain stimulation induces decreased rCBF in the hippocampal formation of the rat. Neuroimage 52:55-61.

Yakushev IY, Dupont E, Buchholz HG, Tillmanns J, Debus F, Cumming P, Heimann A, Fellgiebel A, Luhmann HJ, Landvogt C, Werhahn KJ, Schreckenberger M, Potschka H, Bartenstein P (2010) In vivo imaging of dopamine receptors in a model of temporal lobe epilepsy. Epilepsia 51:415-422.

Yankam Njiwa J, Costes N, Bouillot C, Bouvard S, Fieux S, Becker G, Levigoureux E, Kocevar G, Stamile C, Langlois JB, Bolbos R, Bonnet C, Bezin L, Zimmer L, Hammers A (2016) Quantitative longitudinal imaging of activated microglia as a marker of inflammation in the pilocarpine rat model of epilepsy using [11C]-(R)-PK11195 PET and MRI. J Cereb Blood F Met.

Zhang L, Guo Y, Hu H, Wang J, Liu Z, Gao F (2015) FDG-PET and NeuN-GFAP immunohistochemistry of hippocampus at different phases of the pilocarpine model of temporal lobe epilepsy. Int J Med Sci 12:288-294.

Zhong J, Petroff OA, Prichard JW, Gore JC (1993) Changes in water diffusion and relaxation properties of rat cerebrum during status epilepticus. Magn Reson Med 30:241-246.

Figure captions

Fig. 1. Directionally encoded (DEC) fractional anisotropy diffusion MRI maps of the hippocampus from control (A) and from a rat that had experienced pilocarpine-induced SE 6 months earlier (B). Directions of water diffusion in DEC maps: red, rostral–caudal; green, medial–lateral; blue, dorsal–ventral. Panel (C) summarizes the major connectivity and panel (D) changes that are consistent with alterations in DEC maps. DG, dentate gyrus; l-m, stratum lacunosum-moleculare; sr, stratum radiatum, CA, cornu ammonis; g, granule cell layer; o, stratum oriens; p, stratum pyramidale; oml, outer molecular layer; iml, inner molecular layer; H, hilus. Modified from Sierra et al. (2015).

Fig. 2. A multimodal follow-up of the same animal before (left) and after (right) status epilpticus induced by systemic kainic acid (KA) injection. (A) T2-weighted MRI image from the same rat before and 8 days after injection of KA. Arrow heads point to enlarged ventricels and lesion in piriform cortex. (B) Awake EEG from the same subject during baseline (left) and at day 8 (right) showing clusters of epileptic discharges marked with

asteriks. (C) Functional connectivity matrices before and 8 days after KA injection show altered connectivity pattern. Reproduced from Pirttimaki et al. (2016).

Fig. 3. In the pilocarpine-induced SE model of TLE, Choi and colleagues evaluated the metabolic connectivity based on ^{18}F-FDG PET in the controls and epilepsy rats during chronic epilepsy (4-6 weeks after SE). They applied a multiscale network analysis to determine differences between control and epilepsy rats. This approach identified reduced connectivity (indicated by reduced interregional correlation) in the left amygdala and left entorhinal cortex. In the figure, distance maps for controls (A) and epilepsy (B) models, respectively. (C) To determine statistically significant differences in metabolic connectivity between groups, p-values were calculated for all possible connections using permutation test. (D) The anatomical distribution of significantly different links between groups. In the epilepsy rats, significantly reduced connectivity was found in several pairwise nodes involving the left amygdala and left entorhinal cortex. Modified from Choi et al. (2014a).

Fig. 4. In the KASE rat model of TLE, Bertoglio and colleagues investigated the capability of ^{18}F-PBR111 PET imaging at disease onset to predicts SRS outcome. The authors applied a multivariate data-driven modeling approach on ^{18}F-PBR111 SUV 2 weeks post-SE. Principal component analysis differentiated subpopulations of animals with different seizure burden (A). (B) Differences in SRS experienced by the three subpopulations of KASE animals. $^{**}P < 0.01$. Partial least squares regression accurately predicted SRS frequency for each animal (C). Each circle represents one animal. SRS, spontaneous recurrent seizures. Modified from Bertoglio et al. (2017).

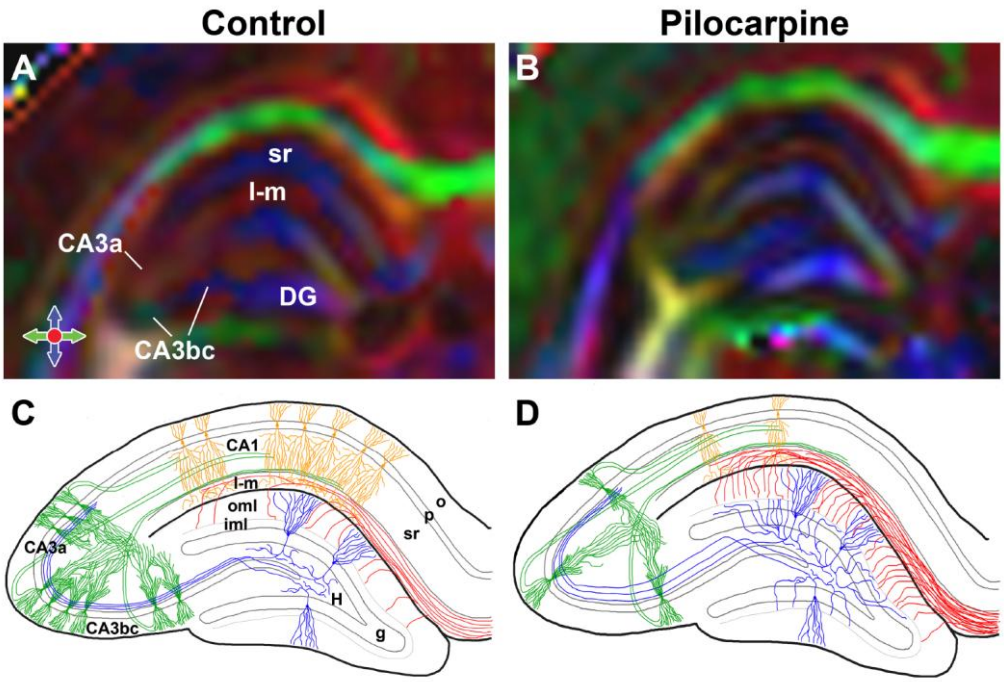

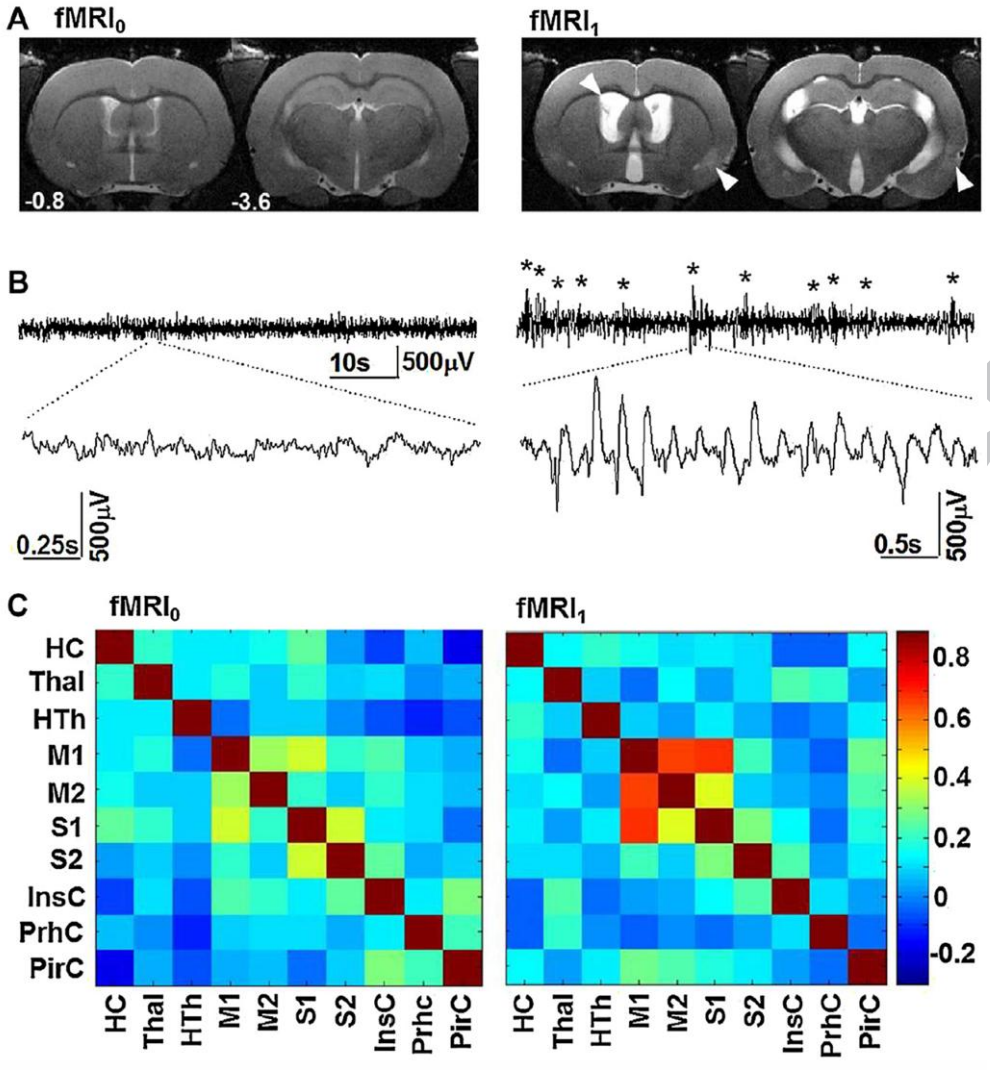

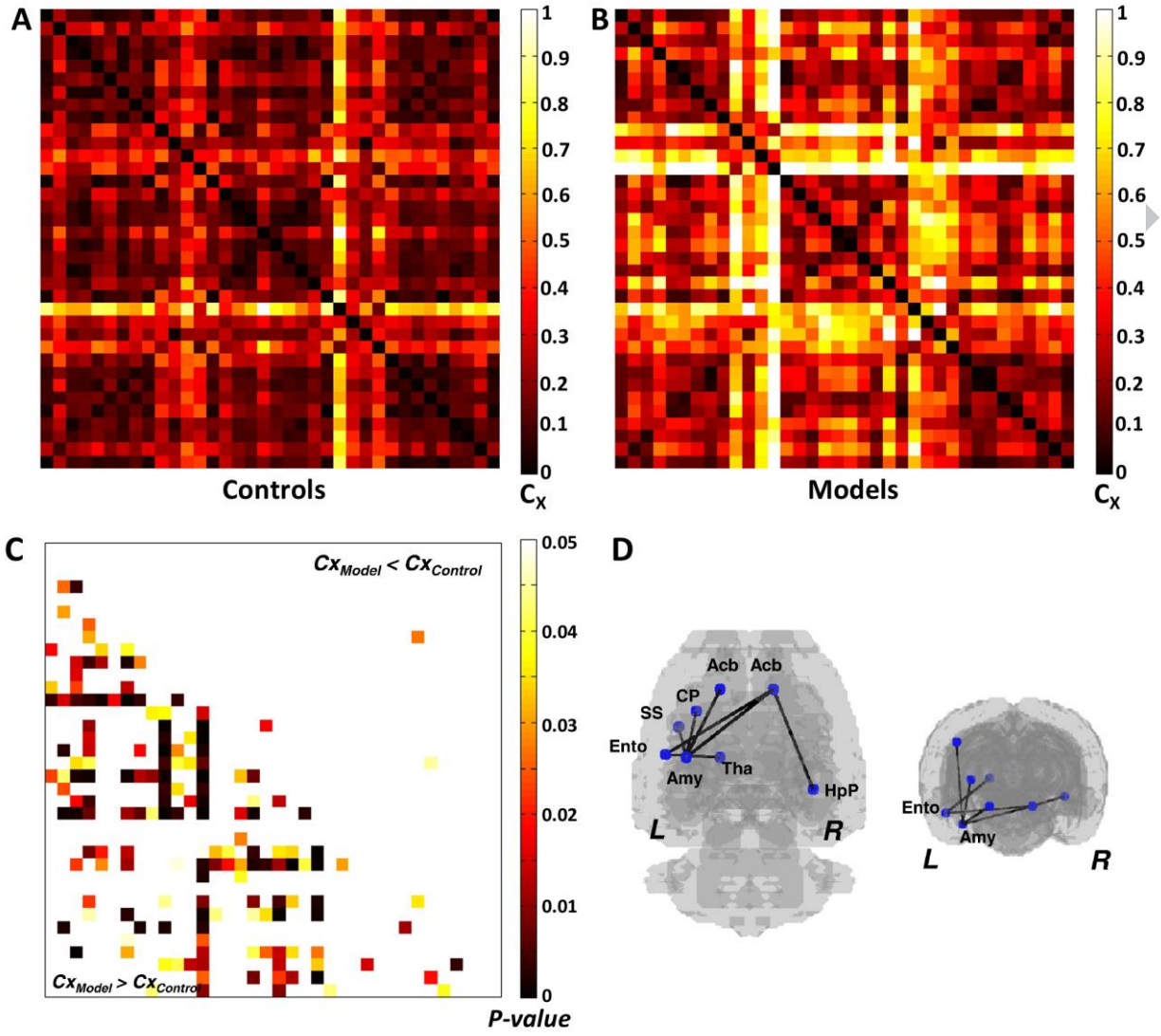

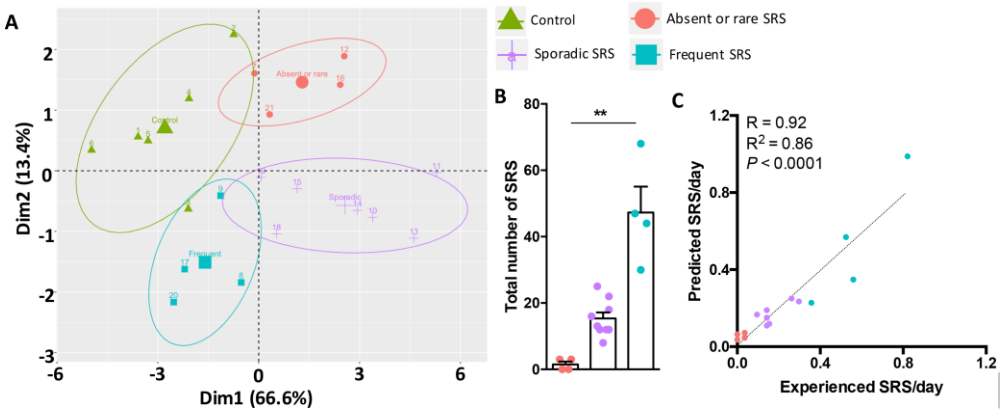

Highlights

- Non-invasive imaging is an important tool for preclinical epilepsy research.
- Neuroimaging represents a translatable technique to identify early biomarkers.
- Longitudinal neuroimaging can improve our knowledge of the process of epileptogenesis.